The pUL51 Tegument Protein Is Essential for Marek's Disease Virus Growth In Vitro and Bears a Function That Is Critical for Pathogenesis In Vivo

David Pasdeloup, Aurélien Chuard, Sylvie Rémy, Katia Courvoisier-Guyader, Caroline Denesvre

AMERICAN SOCIETY FOR MICROBIOLOGY | Journal of Virology®

PATHOGENESIS AND IMMUNITY

The pUL51 Tegument Protein Is Essential for Marek's Disease Virus Growth *In Vitro* and Bears a Function That Is Critical for Pathogenesis *In Vivo*

David Pasdeloup,[a] Aurélien Chuard,[a] Sylvie Rémy,[a] Katia Courvoisier-Guyader,[a] Caroline Denesvre[a]

[a]Laboratory of Biology of Avian Viruses, INRAE-Université de Tours, Nouzilly, France

ABSTRACT pUL51 is a minor tegument protein important for viral assembly and cell-to-cell spread (CCS) but dispensable for replication in cell culture of all Herpesviruses for which its role has been investigated. Here, we show that pUL51 is essential for the growth of Marek's disease virus, an oncogenic alphaherpesvirus of chickens that is strictly cell-associated in cell culture. MDV pUL51 localized to the Golgi apparatus of infected primary skin fibroblasts, as described for other Herpesviruses. However, the protein was also observed at the surface of lipid droplets in infected chicken keratinocytes, hinting at a possible role of this compartment for viral assembly in the unique cell type involved in MDV shedding *in vivo*. Deletion of the C-terminal half of pUL51 or fusion of GFP to either the N- or C-terminus were sufficient to disable the protein's essential function(s). However, a virus with a TAP domain fused at the C-terminus of pUL51 was capable of replication in cell culture, albeit with viral spread reduced by 35% and no localization to lipid droplets. *In vivo*, we observed that although the replication of this virus was moderately impacted, its pathogenesis was strongly impaired. This study describes for the first time the essential role of pUL51 in the biology of a herpesvirus, its association to lipid droplets in a relevant cell type, and its unsuspected role in the pathogenesis of a herpesvirus in its natural host.

IMPORTANCE Viruses usually spread from cell to cell through two mechanisms: cell-released virus and/or cell-to-cell spread (CCS). The molecular determinants of CCS and their importance in the biology of viruses during infection of their natural host are unclear. Marek's disease virus (MDV) is a deadly and highly contagious herpesvirus of chickens that produces no cell-free particles *in vitro*, and therefore, spreads only through CCS in cell culture. Here, we show that viral protein pUL51, an important factor for CCS of Herpesviruses, is essential for MDV growth *in vitro*. We demonstrate that the fusion of a large tag at the C-terminus of the protein is sufficient to moderately impair viral replication *in vivo* and almost completely abolish pathogenesis while only slightly reducing viral growth *in vitro*. This study thus uncovers a role for pUL51 associated with virulence, linked to its C-terminal half, and possibly independent of its essential functions in CCS.

KEYWORDS UL51, herpesvirus, lipid droplet, Marek, pathogenesis

Viruses are transmitted from cell to cell by cellular contacts (cell-to-cell spread or CCS) and/or by infection of a distant cell by extracellular virions. The mode of transmission is usually determined by multiple factors such as the virus itself, but also the infected cell type. CCS has often been overlooked when cell-free particles are available, yet it is admitted as a vital mode of transmission *in vivo* where specific, highly differentiated cell types are involved such as in multilayered epithelia. In the case of *Gallid alphaherpesvirus 2* or Marek's disease virus (MDV), an oncogenic alphaherpesvirus of chickens, this is the exclusive mode of transmission in cell culture because no

Editor Jae U. Jung, Lerner Research Institute, Cleveland Clinic

Address correspondence to David Pasdeloup, david.pasdeloup@inrae.fr.

The authors declare no conflict of interest.

Received 14 February 2023
Accepted 24 March 2023
Published 8 May 2023

free infectious particle can be isolated from the supernatant of infected cells. *In vivo*, MDV infects T-lymphocytes, where it establishes latency, and keratinocytes, where it actively replicates, especially in the feather follicle epithelium (FFE) from where the virus is shed associated with dander and poultry dust (1). Naïve chickens are contaminated by inhalation of this infectious material. It is postulated that keratinocytes are infected through CCS by latently infected T-lymphocytes which locally reactivate in the FFE (2). MDV is therefore an excellent model to understand the molecular mechanisms involved in CCS and their involvement in viral replication *in vivo*.

Among the most important viral proteins described to date as being important for CCS of alphaherpesviruses are the complexes pUL51/pUL7 (3–6) and glycoproteins E and I (gE/gI) (7, 8). Contrary to alphaherpesviruses producing important quantities of extracellular virions such as *Human alphaherpesvirus 1* (or Herpes Simplex Virus 1, HSV-1) or *Suid alphaherpesvirus 1* (Pseudorabies virus, PrV), gE and gI are indispensable for MDV replication in cell culture (9). We therefore focused on pUL51, a protein conserved in all herpesviruses, contrary to gE which is specific of alphaherpesviruses, and that has not been studied until now for MDV. pUL51 is a small minor tegument protein of 249 aa for MDV (3, 6, 10). Although the UL51 gene is conserved in the Herpesvirus family (11), it was reported as nonessential for virus growth in all the viruses in which the gene was deleted or inactivated, even though viral growth was often strongly impaired (3–6, 12–15). pUL51 is involved in secondary envelopment of HSV-1, PrV, *Human alphaherpesvirus 3* (or Varicella-Zoster Virus, VZV), *Bovine alphaherpesvirus 1* (BoHV-1), and *Human betaherpesvirus 5* (or human cytomegalovirus, hCMV) particles (4, 5, 12, 13, 16). Importantly, pUL51 has cell-type specific CCS functions in HSV-1 infected cells (6) which are linked to its interaction with pUL7 (through residues 30 to 90 of pUL51) and its ability to correctly address glycoprotein gE to cell junctions (through the C-terminal half of pUL51) (3, 6, 10, 17). Here, using MDV has a model herpesvirus which entirely depends on CCS as the only route of infection in cell culture, we investigated the role of pUL51 in viral spread *in vitro*, as well as its role *in vivo* in pathogenesis and transmission in the natural host of MDV.

RESULTS

UL51 is indispensable for MDV growth *in vitro*. MDV pUL51 is 249 residues long with the 32 to 159 domain being particularly well conserved with other alphaherpesviruses (Fig. 1). In contrast, the C-terminal half of the protein (160 to 249) is poorly conserved even in the closely related *Gallid alphaherpesvirus 3* (MDV-2). In order to determine the role of UL51 in MDV replication cycle, we inactivated the expression of pUL51 by mutating the methionine codon at position 30 with a stop codon in the viral genome (BAC rUL51M30STOP) (Fig. 1 and 2). Complete deletion of the gene was excluded because of the close proximity of the neighboring UL50 and UL52 genes and of a potential uncharacterized ORF (MDV063.5) overlapping with the terminal 3′ end of UL51 (Fig. 2A). The integrity of genomes was controlled by restriction fragment length polymorphism (RFLP) which showed the expected digestion profiles for all constructs, including those that were not infectious (Fig. 3). Despite several attempts, we were unable to recover infectious virus from chicken embryonic skin cells (CESCs) electroporated with rUL51M30STOP, as opposed to cells electroporated with the control rRB-1B BAC, indicating that the mutation is lethal for viral replication and/or essential for CCS. Similarly, no infectious virus could be recovered upon transfection of MDV genomes coding for pUL51 fused to GFP at its N- or C-terminus (rUL51-GFP or rGFP-UL51) or for a truncated pUL51 lacking the nonconserved C-terminal half (rUL51ΔCt) (Fig. 2B). Immunofluorescence analysis of these four mutants showed the presence of individual cells positive for MDV antigens (Fig. 4), which excludes a failure of transfection and rather indicates that the viral cycle is abortive with these viruses. However, viruses harboring a C-terminal fusion of either the tandem affinity purification (TAP) tag or the strep-tag-HA (SHA) tag on pUL51 could be recovered and were named vUL51TAP and vUL51SHA, respectively (Fig. 2B). The TAP tag is 183 aa long whereas the size of the SHA tag is minimal (17 aa). Both tags were initially added to pUL51 to allow for the purification of protein complexes from lysates

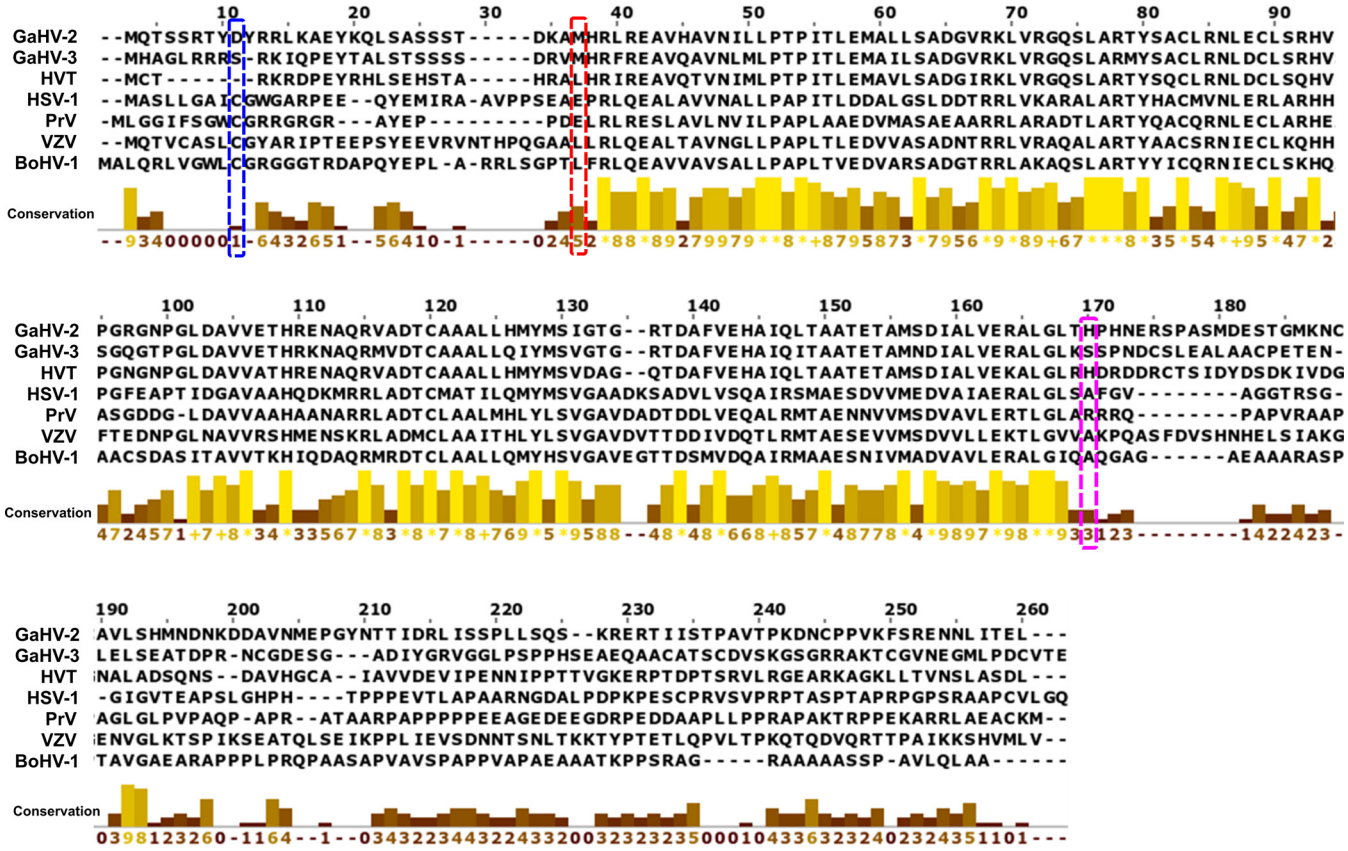

FIG 1 Sequence alignment of MDV pUL51 with other alphaherpesviruses. The protein sequence of pUL51 from MDV (top line, GaHV-2) was compared with the corresponding protein from (top to bottom): *Gallid alphaherpesvirus 3* (GaHV-3), *Meleagrid alphaherpesvirus 1* (Herpesvirus of Turkey, HVT), *Human alphaherpesvirus 1* (Herpes Simplex Virus 1, HSV-1), *Suid alphaherpesvirus 1* (Pseudorabies Virus, PrV), *Human alphaherpesvirus 3* (Varicella-Zoster Virus, VZV), and *Bovine alphaherpesvirus 1* (Infectious Bovine rhinotracheitis virus, BoHV-1). The conservation score is indicated below the alignment. Residues that were mutated into a STOP codon in MDV-1 rUL51M30STOP (Met30) and in rUL51ΔCt (His 161) are highlighted by a red and a pink box, respectively. A conserved cysteine in alphaherpesviruses but not in most of Mardiviruses is highlighted by a blue box.

obtained from cell culture or infected animal tissues. The presence of a hypothetical ORF (MDV063.5) overlapping the 3′ terminal end of the UL51 ORF where the TAP fusion is present made it necessary to generate a control virus in which the TAP coding sequence would be kept but where the fusion with pUL51 would be lost. We thus generated the vUL51TAPiSTOP virus where a STOP codon was introduced in between the UL51 and the TAP ORFs (Fig. 2). The expression of neighboring genes UL50 and UL52 was unaffected by this modification in cells infected with vUL51TAP or vUL51TAPiSTOP, as assessed by RT-PCR (Fig. 5A). The viral growth properties of vUL51TAP and vUL51TAPiSTOP in CESCs were compared to vTK_TAP, a virus encoding the TAP tag alone under the dependence of the thymidine kinase (TK) promoter. This showed that while there was no difference in growth properties between vTK_TAP and vUL51TAPiSTOP, the size of vUL51TAP plaques were about 35% smaller than those of vUL51TAPiSTOP or vTK_TAP (Fig. 5B and C). Thus, the TAP fusion at the C-terminus of pUL51 affected a function of pUL51 which resulted in altered CCS and/or replication. This effect was independent of the genomic presence of the TAP sequence at the 3′-end of UL51, as showed by the normal size of vUL51TAPiSTOP plaques. The fusion of the TAP tag to pUL51 and the expression of the resulting protein were verified by Western blotting (Fig. 5D). The TAP tag contains two protein A domains which can bind to immunoglobulins. Therefore, the TAP tag could be detected in infected cell lysates using a rabbit horseradish peroxidase-conjugated antibody. This showed that a protein of the expected size for the UL51TAP fusion (~47 kDa) was present in the vUL51TAP cell lysates, whereas a protein of ~20 kDa was detected in the vTK_TAP cell lysates, corresponding to the expected size for the TAP tag alone. No protein was detected in the vUL51TAPiSTOP cell lysate, whereas major capsid protein VP5 was present

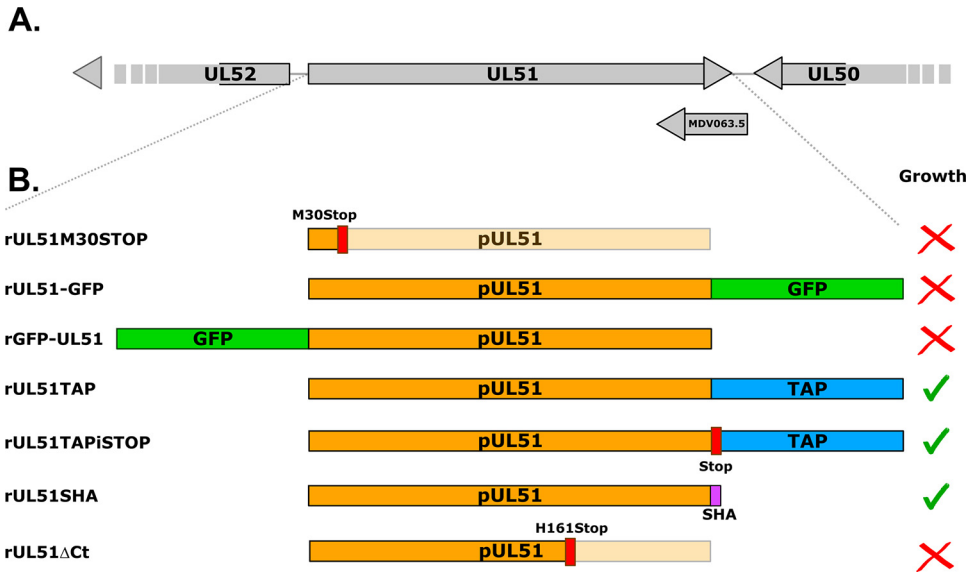

FIG 2 Constructions used in this study. (A) Representation of the UL51 locus with neighboring genes. The direction of the locus has been inverted for better readability. A putative ORF (MDV063.5) overlaps with the end of the UL51 ORF. (B) Summary of constructs used in this study with the corresponding modifications on pUL51. Growth in cell culture is indicated by a green check mark whereas absence of growth is indicated by a red cross. rTK_TAP and rTK_GFP-SHA and rUL51ΔCt-repair are not represented here since they do not have any alteration on UL51.

in all cell lysates. This demonstrates that the UL51TAP fusion is properly expressed in vUL51TAP infected cells whereas the TAP tag is not expressed either alone or in association with pUL51 in vUL51TAPiSTOP infected cells. Contrary to vUL51TAP, the growth properties of vUL51SHA were comparable to those of the vTK_GFP-SHA control virus, which encodes the SHA tag fused to the GFP expressed under the dependence of the TK promoter (Fig. 5A and B). Taken together with the absence of recovery of vUL51GFP, this indicates that the impairment of the pUL51 function is dependent on the nature of the tag fused at its C-terminus.

MDV pUL51 cellular localization. Several reports showed that pUL51 has a conserved affinity for cellular membranes, in particular for those from the Golgi apparatus (3–6, 18, 19). In order to compare these observations to pUL51 MDV, we investigated the localization of the protein in transfected and infected cells. A plasmid encoding pUL51 fused to a C-terminal V5 tag was transfected into the chicken cell line ESCDL-1 and, to our surprise, pUL51 localized to mitochondria (Fig. 6A). When pUL51 was co-expressed with its binding partner pUL7, localization of pUL51 changed from mitochondrial to very nuclear and cytoplasmic (Fig. 6B). A similar phenotype was observed when the conserved N-terminal half (1-159) of pUL51 was expressed. Contrary to pUL51 full-length or pUL51 1–159, the localization of the nonconserved C-terminal half (160-end) of pUL51 was not mitochondrial and it was not affected by the presence of pUL7. This indicates that the N-terminal half of pUL51 is sufficient for mitochondrial localization, that it likely bears the interaction domain of pUL7, as is expected from studies on HSV-1 (3, 10, 17, 20), and that this interaction influences the localization of pUL51. The mitochondrial localization of pUL51 was not dependent on the nature of the tag since pUL51 fused to a C-terminal myc tag also localized to mitochondria (Fig. 7A). pUL51-myc displayed a nucleo-cytoplasmic localization when co-expressed with pUL7 as was observed with pUL51-V5 (Fig. 7A). Mitochondrial localization of pUL51 was also not restricted to ESCDL-1 cells because pUL51-myc was also localized in the mitochondria of electroporated CESCs and not in the Golgi apparatus (Fig. 7B). However, in CESCs infected by vUL51SHA, pUL51 localized to the Golgi (Fig. 7C). These results show that pUL51 of MDV depends on other viral factors to localize to the Golgi and that pUL7 is not sufficient for this localization.

The experiment was reproduced in chicken keratinocytes derived from embryonic stem cells (21). Chicken keratinocytes from the feather follicle epithelium represent the cellular

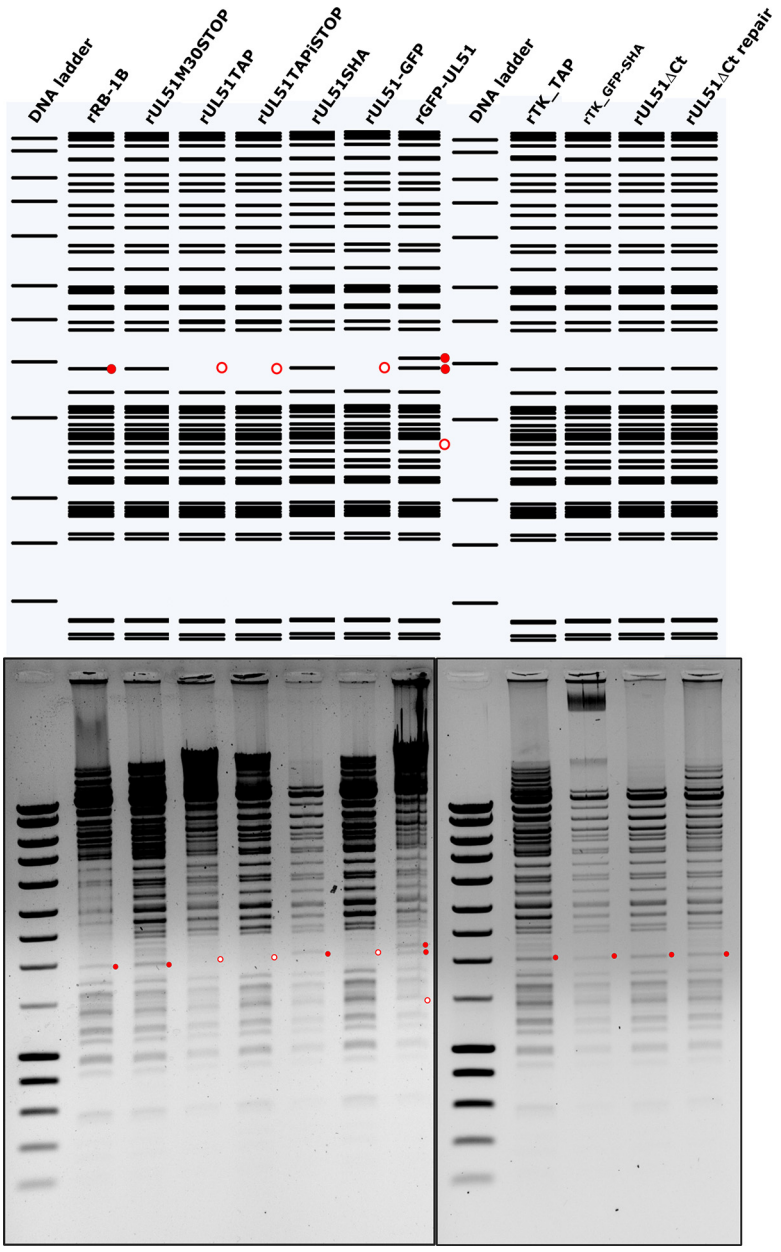

FIG 3 RFLP analysis of all genomes used in this study. 1 μg of purified BACs were digested with NdeI. The digestion profiles were analyzed on a 0.6% TBE agarose gel (bottom) and compared to the corresponding expected profiles (top). The DNA ladder used is SmartLadder (Eurogentec). Red dots indicate specific bands.

type in which MDV replication is the most active *in vivo* and from where the virus is shed into the environment (1, 22). Unlike mammals, avian keratinocytes contain lipid droplets which contribute to the impermeability of the skin in the absence of sebaceous glands (23). We observed that pUL51 was localized at the surface of lipid droplets in keratinocytes that were transfected with a plasmid encoding pUL51-myc independently of the expression of pUL7, which did not localize to lipid droplets (Fig. 8). In vUL51SHA-infected keratinocytes, pUL51 localized to lipid droplets (Fig. 9A), although the localization to lipid droplets was less pronounced and common than in transfected cells, in part because of the low expression of UL51 during infection. This localization was specific to pUL51 because VP22, another tegument protein, did not localize to lipid droplets (Fig. 9B). Altogether, these results confirm the affinity of pUL51 for the Golgi apparatus in infected cells, and they show that pUL51 can also be localized in a lipid-rich compartment (the lipid droplets) of

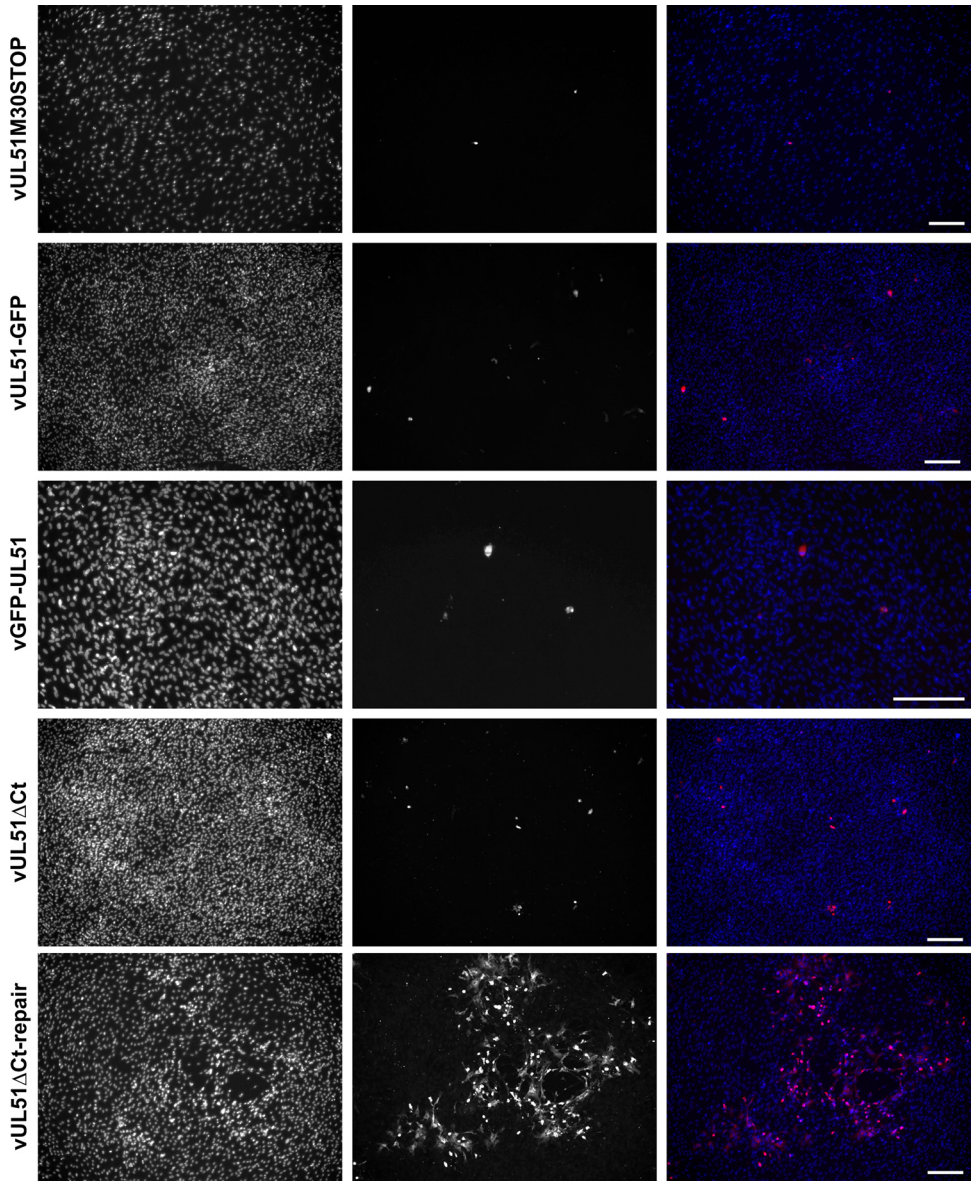

FIG 4 Detection of viral antigens in CESCs transfected with non-infectious BACs. CESCs were electroporated with 4 μg of BAC DNA. Four days later, cells were fixed, permeabilized, and viral antigens were detected using three different monoclonal antibodies specific of ICP4, glycoprotein gB and VP22 and a goat anti-mouse Alexa Fluor 555-conjugated secondary antibody (red). Nuclei were counterstained with Hoescht. Note the presence of individually infected cells in all non-infectious BACs, as opposed to the presence of viral plaques in cells transfected with rUL51ΔCt-repair. Scale bars: 200 μm.

avian keratinocytes, a highly specialized epithelial cell type which is biologically relevant for MDV replication and shedding.

Replication and phenotype of vUL51TAP and vUL51TAPiSTOP in chickens. As it was impossible to obtain a UL51-null virus, we used the moderately defective vUL51TAP in order to evaluate the role of pUL51 in viral replication and pathogenesis *in vivo*, using vUL51TAPiSTOP as a control. A total of 2,000 PFU (plaque-forming units) of either virus were inoculated by intramuscular route to 10 White Leghorn chickens of 2 weeks of age. Five naive contact chickens were added to each group to test for the horizontal transmission of the virus. As shown in Fig. 10A, by the end of the experiment (70 days postinoculation [pi]), 70% of animals inoculated with vUL51TAPiSTOP had developed clinical signs of Marek's disease and were euthanized with a median of survival of 47 days, as opposed to none in the vUL51TAP group. Similarly, while 50% of contact animals developed clinical

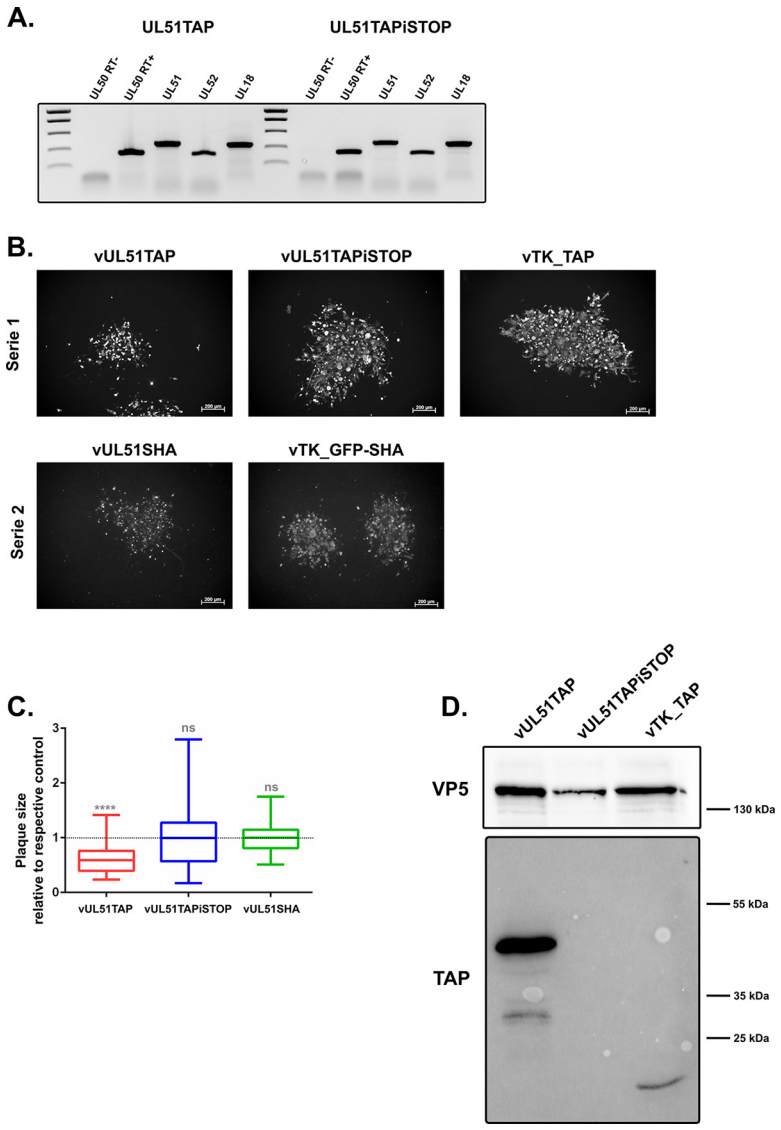

FIG 5 Viral expression and spread of TAP constructs. (A) Expression of genes neighboring UL51 in cells infected with vUL51TAP or vUL51TAPiSTOP. RNA was extracted from CESCs infected with vUL51TAP or vUL51TAPiSTOP for 5 days and RT-PCRs were carried out using primers specific for UL50, UL51, and UL52. UL18 was used as a control gene for infection. RT(+) and RT(-) in the UL50 condition indicates whether reverse transcriptase was added to the mix or not, respectively. (B and C) The area of individual plaques of vUL51TAP, vUL51TAPiSTOP, vTK_TAP, vUL51SHA, and vTK_GFP-SHA were measured 4 days postinfection on chicken primary embryonic skin cells (CESCs). (B) Viral plaques were visualized using a mix of monoclonal antibodies directed against ICP4, VP22, and gB. Plaques from two independent experiments are shown, one for the TAP-tagged viruses (Serie 1) and one for the SHA-tagged viruses (Serie 2). Scale bars: 200 μm. (C) The area of a minimum of 50 plaques was measured for each virus and the median of plaque size for each virus is shown respective of its corresponding control (median of vTK_TAP and vTK_GFP-SHA plaque size set as 1 for all TAP viruses and vUL51SHA, respectively). Results are shown as box plots. Significant differences in plaque areas were determined using a one-way ANOVA with Dunett's test (comparison of vUL51TAP and vUL51TAPiSTOP to the vTK_TAP control) or Tukey's test (comparison of vUL51SHA to its vTK_GFP-SHA control). ns, not significant; ($P > 0.5$); ****, $P < 0.0001$. (D) Western-blot showing the detection of the TAP fusion proteins using a rabbit anti-goat horseradish peroxidase antibody (lower panel) and the detection of the major capsid protein VP5 as a control of infection (upper panel). Molecular weight ladder is depicted on the right of each picture.

signs and were euthanized by 70 days post-infection (dpi) in the vUL51TAPiSTOP group, none of the animals from the vUL51TAP group displayed any symptom of the disease. Necropsy revealed that none of the animals from the vUL51TAP group, whether inoculated or contact, had tumors except one inoculated chicken. In contrast, 90% of animals inoculated with vUL51TAPiSTOP, including surviving animals, had tumors. This shows that

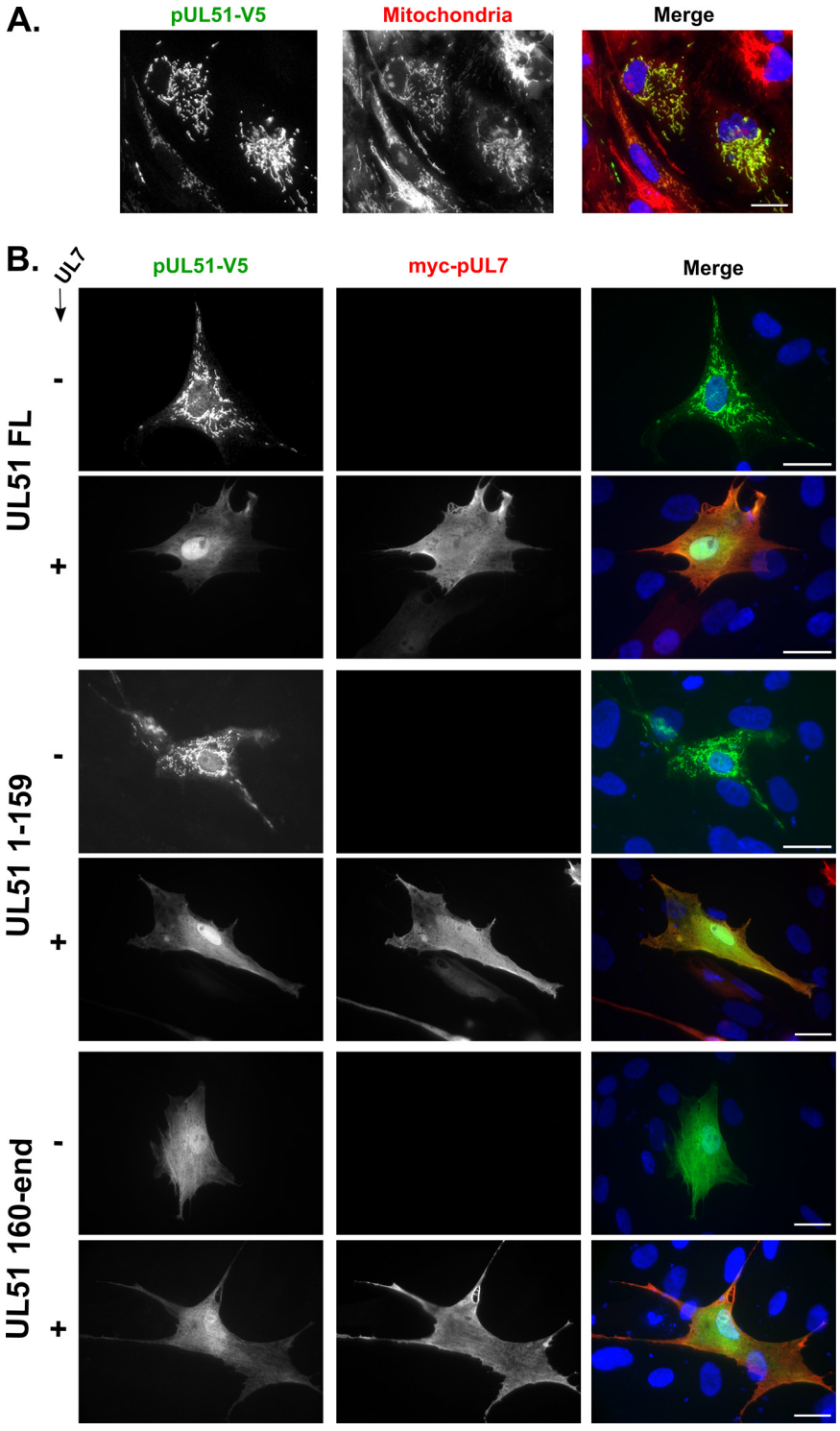

FIG 6 pUL51 intracellular localization in transfected ESCDL-1. ESCDL-1 cells were transfected with a plasmid encoding pUL51-V5 full-length or the 1 to 159 or the 160-end fragments associated to a C-terminal V5 tag. (A) Cells were stained with Mitotracker Orange to label mitochondria (red) and with an anti-V5 antibody to label pUL51 (green). (B) Cells were transfected with plasmids encoding the different UL51 constructs and were co-transfected (+) or not (−) with a plasmid encoding pUL7-myc. Then, 24 h later, cells were labeled with an anti-V5 antibody to visualize pUL51 (green) and with an anti-myc antibody to label pUL7 (red). All cells were counterstained with Hoescht to label nuclei (blue). Scale bars, 20 μm.

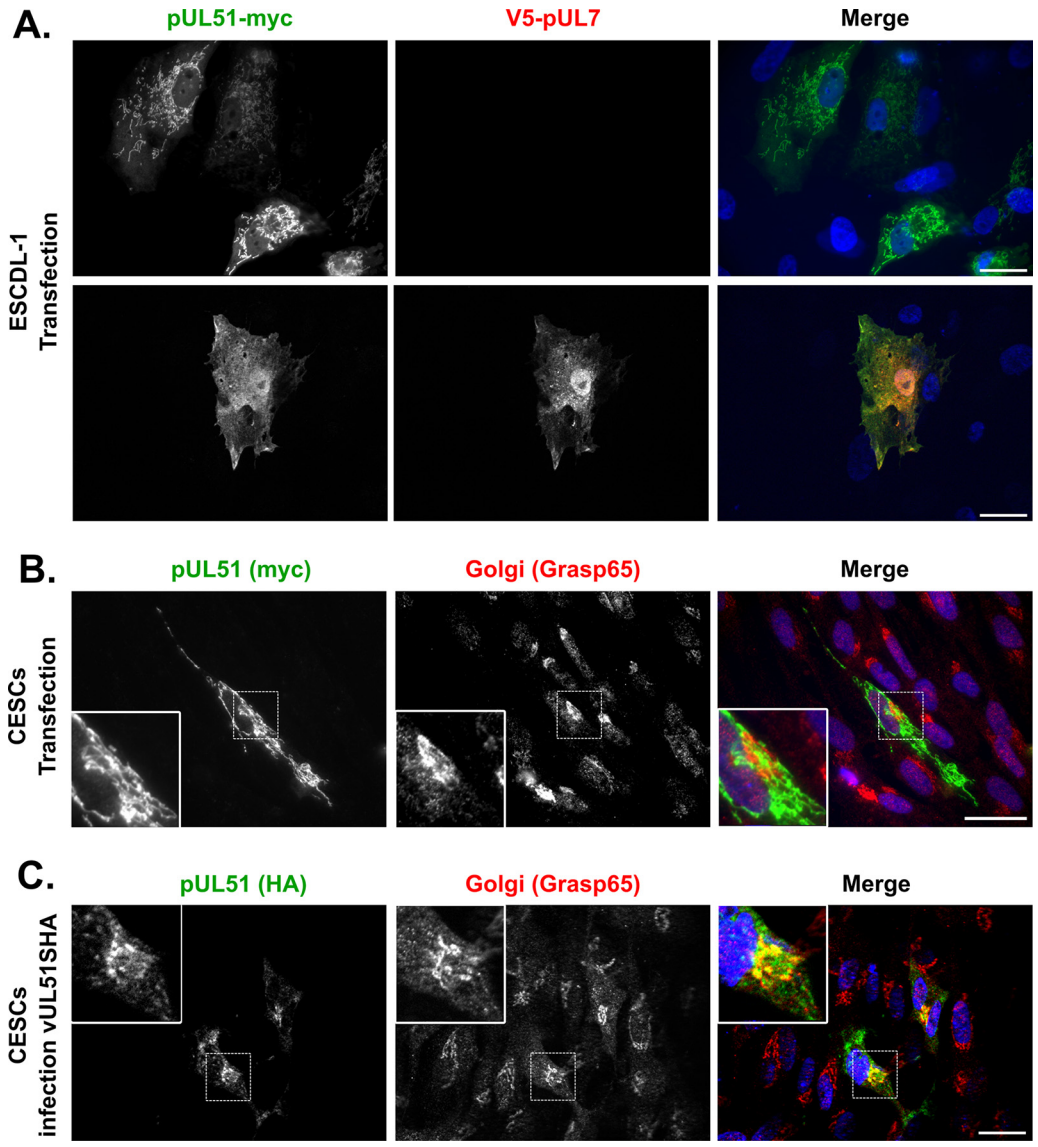

FIG 7 pUL51 intracellular localization in transfected ESCDL-1 and transfected or infected CESCs. (A) ESCDL-1 were transfected with a plasmid encoding pUL51-myc with or without a plasmid encoding V5-pUL7. Cells were labeled with an anti-myc antibody to visualize pUL51 (green) and with an anti-V5 antibody to visualize pUL7 (red). (B and C) CESCs were either transfected with a plasmid encoding pUL51-myc (B) or infected with vUL51SHA (C). Cells were stained with an anti-grasp65 to label the Golgi apparatus (red) and with an anti-myc (B) or an anti-HA antibody (C) to label pUL51 (green). All cells were counterstained with Hoescht to label nuclei (blue). An area (dashed box) is enlarged 2.5 times to better show pUL51 localization. Scale bars, 20 μm.

the function(s) impaired by the TAP fusion at the C-terminus of pUL51 is (are) essential for pathogenesis but that the mutation is not sufficient to completely abolish tumorigenesis. Viral replication kinetics were similar between the two viruses with a peak of viral replication observed at 28 dpi in peripheral blood mononuclear cells (PBMC) and 21 dpi in feathers (Fig. 10B and 10C). However, viral genome loads in PBMCs and in feathers of vUL51TAP-infected animals were up to 60 times lower than those of vUL51TAPiSTOP-infected animals (Fig. 10B and C) with a median of 17 times lower in PBMC and 27 times lower in feathers (Fig. 10D), although differences were significant essentially at the peak of viral replication (21 to 35 dpi) (Fig. 10B and C). We conclude that although the replication of vUL51TAP is impaired in both lymphocytes and FFE, this defect in viral replication is rather moderate in comparison to the almost complete absence of pathogenesis.

Shedding and horizontal transmission of vUL51TAP and vUL51TAPiSTOP. Given that no symptoms of Marek's disease were observed in contact animals from the

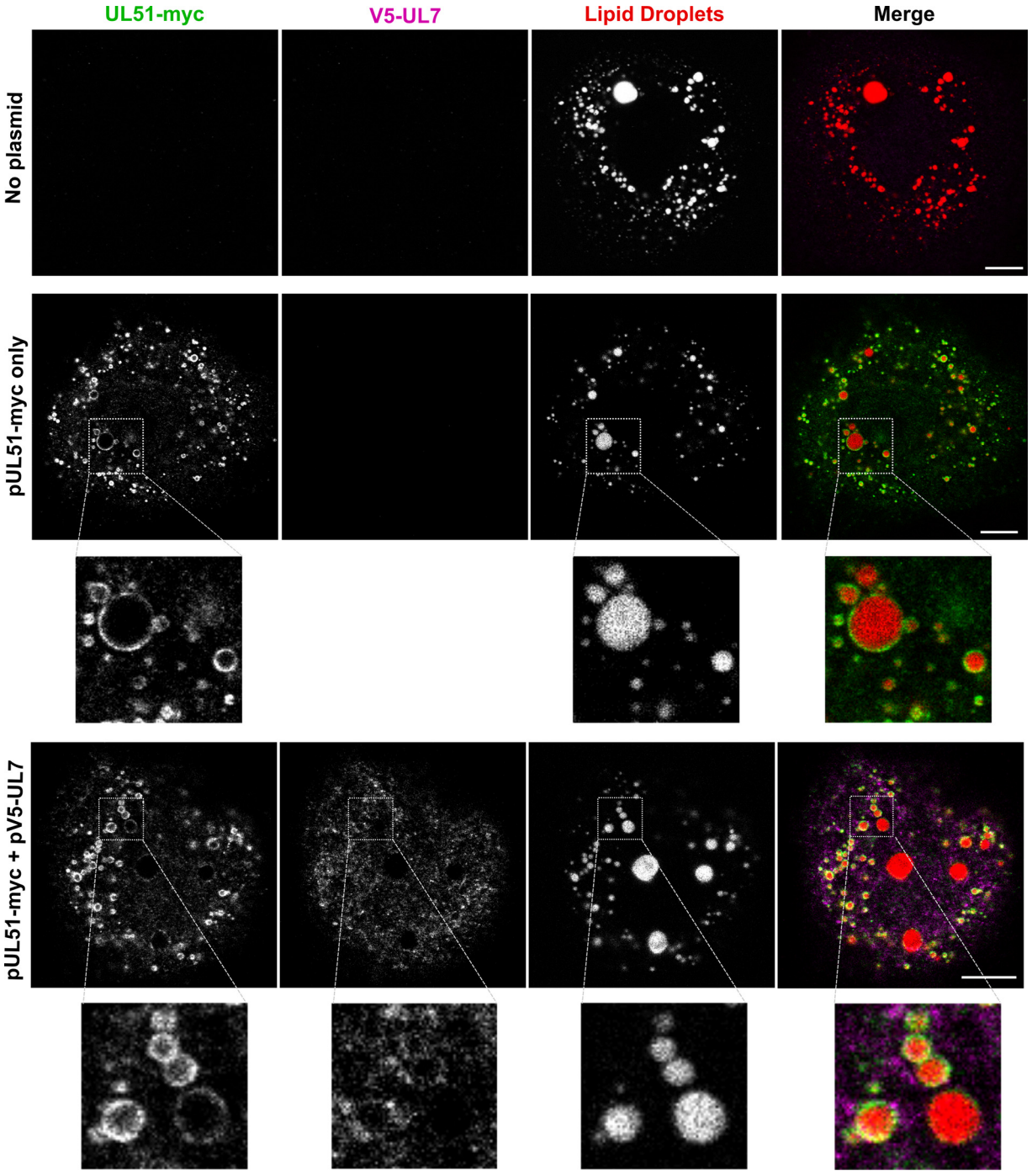

FIG 8 pUL51 intracellular localization in transfected keratinocytes. Keratinocytes were mock-transfected or transfected with a plasmid encoding pUL51-myc either alone or with a plasmid encoding pV5-UL7. Cells were stained with an anti-myc antibody to label pUL51 (green) and an anti-V5 antibody to label pUL7 (magenta). Lipid droplets were visualized through BODIPY 493/503 staining (pseudo-colored in red). Areas in dashed boxes were enlarged 3 to 3.5 times to better show pUL51 localization. Scale bars, 10 μm.

UL51TAP group, genomic viral loads were analyzed and quantified from the PBMC of the contact animals and from the dust accumulated in the housing units in the course of 7 days to check whether animals were infected and whether viral shedding occurred (Fig. 11). Viral loads in the PBMCs of contact animals in vUL51TAP and vUL51TAPiSTOP groups were equivalent to those of the corresponding inoculated animals i.e., low in vUL51TAP animals (less than 10^4 copies per million cells) and high in vUL51TAPiSTOP animals (up to 10^6 copies per million cells) (Fig. 11A, compared with Fig. 10B). In the

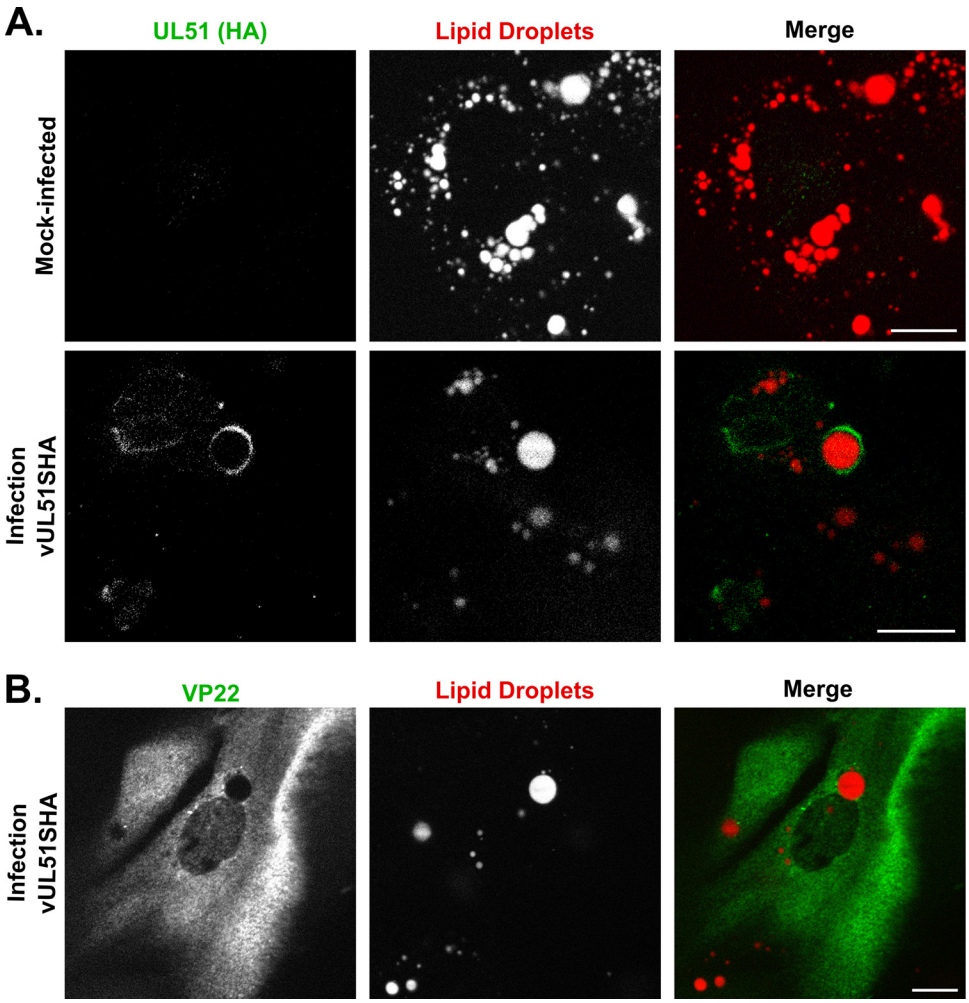

FIG 9 pUL51 intracellular localization in vUL51SHA-infected keratinocytes. Keratinocytes were mock-infected or infected with vUL51SHA for 5 days before fixation. Cells were stained with an anti-HA antibody to label pUL51 (A, green) or an anti-VP22 antibody to label VP22 (B, green). Lipid droplets were visualized through BODIPY 493/503 staining (pseudo-colored in red). Scale bars, 10 μm.

vUL51TAP contact group, viral loads were beneath or close to the detection threshold for three out of five animals, respectively. In the other two animals, viral loads were comparable to those observed in the inoculated animals, showing that transmission occurs, albeit to limited levels probably because of the low viral loads present in the environment. To verify this hypothesis, viral genomes accumulated in the dust of housing units between 21 and 28 dpi and during the last 7 days of experimentation were quantified (Fig. 11B). In the vUL51TAPiSTOP unit, viral genome loads were 2.10^8 and 5.10^8 copies/million cells at 28 dpi and 70 dpi, respectively, whereas they were around 10 times lower at 10^7 and 5.10^7 copies/million cells in the vUL51TAP units. Taken together, these results demonstrate that, although vUL51TAP was impaired in replication, pathogenesis, and viral shedding, infection of contact animals still occurred. Therefore, vUL51TAP is not impaired in horizontal transmission between chickens.

Localization of UL51TAP in transfected and infected cells. pUL51 has a possible role in the final stages of viral assembly such as secondary envelopment (4, 5, 12, 13, 16). Because the fusion of the TAP tag at the C-terminus of pUL51 strongly affects viral pathogenesis *in vivo*, we further studied the cellular localization of the protein in comparison to pUL51 with no TAP tag. Upon transfection of CESCs with a plasmid expressing UL51TAP, pUL51TAP localized to mitochondria but relocalized to the nucleus and the cytoplasm in the presence of pUL7 with partial colocalization between the two

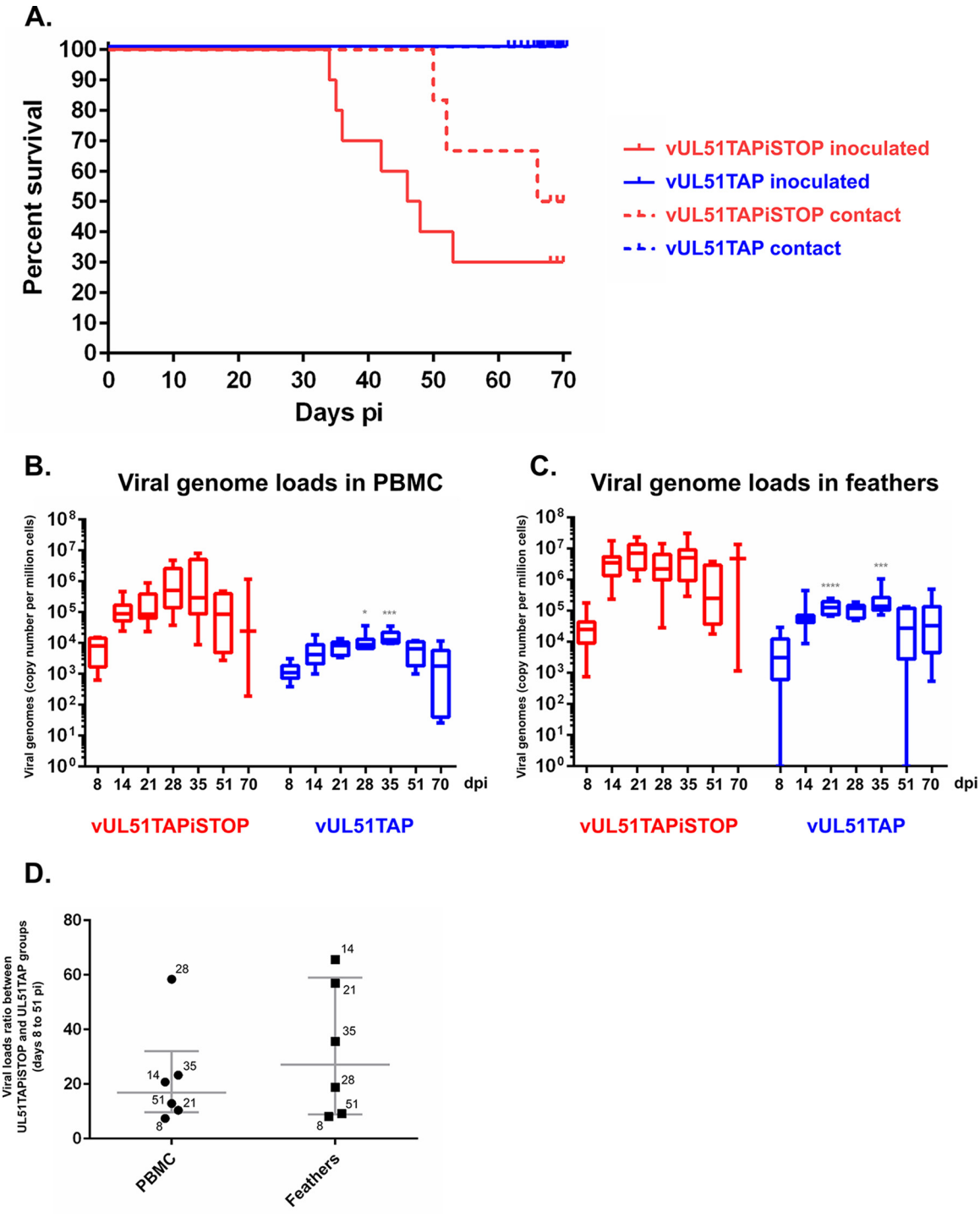

FIG 10 Replication and pathogenesis of vUL51TAP and vUL51TAPiSTOP. (A) Ten 2-week-old white Leghorn chickens were inoculated with 2,000 PFU of vUL51TAP or vUL51TAPiSTOP. The percentage of live animals is shown for vUL51TAP-inoculated (plain blue line) or contact animals (dashed blue line) and vUL51TAPiSTOP-inoculated (plain red line) or contact animals (dashed red line). Animals with apparent symptoms of Marek's disease were euthanized to limit suffering. (B and C) DNA was extracted from PBMC (B) or feathers (C) of chickens inoculated with vUL51TAPiSTOP (in red) or vUL51TAP (in blue) at 8, 14, 21, 28, 35, 51, and 70 days postinoculation. Viral genomes were quantified by real-time quantitative PCR and their numbers are indicated as per million cells. Significance of differences of viral loads in vUL51TAPiSTOP-infected birds and those in vUL51TAP-infected birds were determined using a one-way ANOVA with Sidak's test. Only significant differences are indicated: *, $P < 0.05$; **, $P < 0.01$; ***, $P < 0.001$; ****, $P < 0.0001$. (D) The ratio between the median of viral genome loads of inoculated chickens from the vUL51TAPiSTOP group and the vUL51TAP is shown for each time point (8, 14, 21, 28, 35, and 51 dpi). Results are indicated as a median with interquartile range (box) and minimal and maximal values (whiskers) for PBMCs (left) or feathers (right). Numbers beside individual spots indicate the time point of the sample (days postinfection).

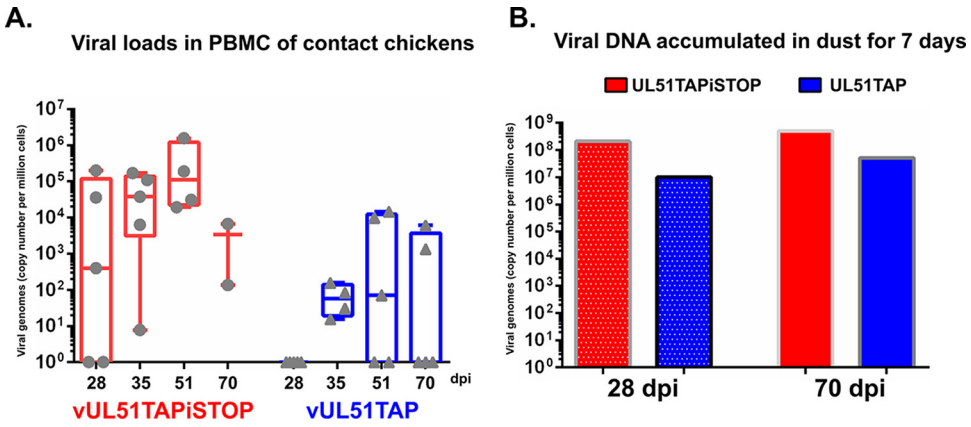

FIG 11 Transmission and excretion of vUL51TAP and vUL51TAPiSTOP. (A) Viral genomes from the PBMCs of contact chickens from the vUL51TAPiSTOP group (red) and the vUL51TAP group (blue) extracted at 28, 35, 51, and 70 dpi were quantified by real-time quantitative PCR and their numbers are indicated as per million of cells. Results are showed as medians with interquartile range (box) and minimal and maximal values (whiskers). The individual values are shown as circles (vUL51TAPiSTOP) or triangles (vUL51TAP). (B) The amount of viral genomes from DNA extracted from the dust accumulated during 1 week (between days 21 and 28 pi and between days 63 and 70 pi, noted "28dpi" and "70dpi," respectively) and collected from the two separate isolators (vUL51TAP in blue, vUL51TAPiSTOP in red) was determined by qPCR. Results are indicated as per million cells.

proteins (Fig. 12A). This pattern of localization was identical to that observed with pUL51 (Fig. 6A and B), indicating that the TAP fusion does not alter this property. In keratinocytes, pUL51TAP localized essentially to mitochondria when expressed alone with occasional and partial localization to lipid droplets (Fig. 12B). The protein relocalized to the cytoplasm when co-expressed with pUL7 with little if any colocalization between the two proteins and no localization to lipid droplets (Fig. 12B). In infected cells, pUL51TAP localized to the Golgi apparatus in CESCs and juxtaposed to Golgi vesicles in keratinocytes (Fig. 12C). Notably, no localization to lipid droplets could be observed. These results show that the fusion of the TAP tag to pUL51 does not impair its interaction with pUL7 or its cellular localization in CESCs. However, contrary to unmodified pUL51, only occasional and partial localization on lipid droplets was observed with pUL51TAP and only in the absence of pUL7 in transfected keratinocytes. Similarly, UL51TAP was not found on droplets in infected cells. Therefore, the fusion of the TAP tag has little effect on the Golgi localization of pUL51, but it affects its localization to lipid droplets in keratinocytes.

DISCUSSION

pUL51 is a minor tegument protein conserved in all Herpesviruses. Although its absence strongly impacts virus yields, it is dispensable for all viruses where its role has been tested (Table 1). For these viruses, pUL51 was shown to be important for secondary envelopment, its deletion resulting in the accumulation of capsids lacking totally or partially their secondary envelope (3, 4, 6, 12–14, 16). In addition, Butt et al. showed that the N-terminal half of HSV-1 pUL51 can adopt a fold resembling that of CHMP4B, a member of the ESCRT-III family of proteins, and that pUL51 can form similar filaments *in vitro*, thus suggesting a role for pUL51 to promote membrane scission during envelopment (20).

A particular feature of interest is the role of pUL51 in CCS in epithelial cell types (6). In cell culture, CCS is the only route of infection possible for MDV. We therefore investigated the role of pUL51 in the spread of MDV and found that, contrary to other Herpesviruses, the protein is essential for viral growth of MDV in cell culture. This would imply that pUL51 is a vital component of the viral machinery for CCS, possibly linked to its function with secondary envelopment.

The affinity of pUL51 for membranes was suspected based on a conserved palmitoylated cysteine within the first 10 residues of the protein (Cys9 for HSV-1). It was shown that

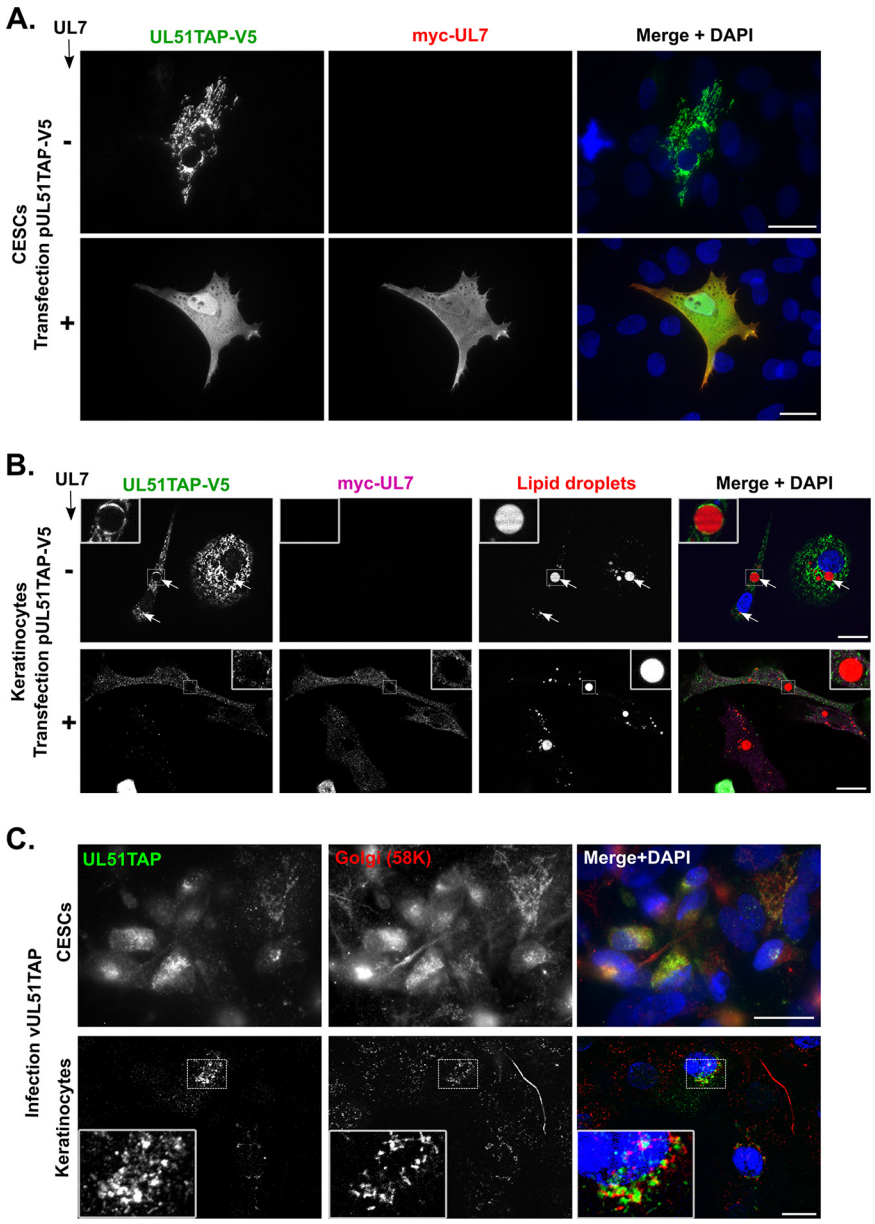

FIG 12 Localization of pUL51TAP in transfected or infected CESCs and keratinocytes. CESCs (A) or keratinocytes (B) were transfected with a plasmid encoding pUL51TAP-V5 in the presence (+) or absence (−) of a plasmid encoding pMyc-UL7 or infected with vUL51TAP for 5 days (C). (A) pUL51TAP was visualized using an anti-V5 rabbit antibody and a goat anti-rabbit Alexa 488-conjugated secondary antibody (green). Cells were then treated with goat serum to saturate all remaining TAP sites before using a mouse anti-myc antibody and goat anti-mouse Alexa 594-conjugated secondary antibody to label pUL7 (red). (B) pUL51TAP was visualized using an anti-V5 rabbit antibody and a goat anti-rabbit Alexa 555-conjugated secondary antibody (pseudo-colored in green). Cells were then treated with goat serum to saturate all remaining TAP sites before using a mouse anti-myc antibody and goat anti-mouse Alexa 647-conjugated secondary antibody to label pUL7 (magenta). BODIPY 493/503 was used to visualize lipid droplets (pseudo-colored in red). (C) UL51TAP was labeled directly using a rabbit anti-goat Alexa 594-conjugated antibody (pseudo-colored in green) and a mouse anti-58K antibody coupled with a goat anti-mouse Alexa Fluor 488-conjugated antibody were used to label the Golgi apparatus (red). An area (dashed box) is enlarged three times to better show pUL51 localization. Scale bars, 20 μm.

the protein localizes on Golgi membranes, that this palmitoylated cysteine is necessary for the Golgi localization of HSV-1 pUL51, and that pUL51 is protected from proteases in the absence of detergent in infected cells (5). Interestingly, the conserved palmitoylated cysteine is not present in MDV pUL51 (blue box in Fig. 1) and we did not observe a Golgi localization of MDV pUL51 upon transfection of chicken cells (Fig. 6A and 7A). In addition, the

TABLE 1 Summary of growth properties of some mutants of pUL51 and its orthologues in different Herpesviruses

Virus	Alteration on UL51	Growth in cell culture	Plaque size	Ref
MDV vUL51M1STOP	No expression	No	NA[d]	This study
MDV vUL51-GFP	GFP fused on Ct	No	NA	This study
MDV GFP-UL51	GFP fused on Nt	No	NA	This study
MDV UL51TAP	TAP fused on Ct	Yes	−35%[a]	This study
MDV UL51//TAP	No alteration[b]	Yes	NS[a]	This study
MDV UL51ΔCt	STOP codon at pos. 161 (Δ161-249)	No	NA	This study
MDV UL51ΔCt-repair	WT sequence restored	Yes	NA	This study
PRV ΔUL51F	Deletion of codons 68 to 233	Yes	−70%	4
HSV1 FDL51	Deletion of codons 42 to 244	Yes	−80%[c]	5
HSV1 UL51Δ73–244	Deletion of codons 73 to 244	Yes	−90% on Vero	6
HSV1 ΔpUL51	Complete deletion except 1 to 23	Yes	approx. −70%	3
VZV-7D	Complete deletion	Yes	Altered	12
BoHV-1 UL51Δ76-232	Deletion of codons 76 to 232	Yes	−90%	13
hCMV TBstop71	Complete deletion except 1 to 12	Yes	−80%	14
EBV dBSRF1-stop	Complete deletion except 1 to 39	Yes	Not tested	15

[a]Compared to vTK_TAP (Fig. 5).
[b]TAP ORF separated from UL51 ORF by STOP codon.
[c]Estimated from Fig. 5.
[d]NS, not significant; NA = not applicable.

pUL51-pUL7 complex from MDV does not localize to the Golgi in transfected cells contrary to HSV-1, VZV, or hCMV homologues (20); although, pUL51 localizes to the Golgi of infected primary chicken skin fibroblasts (Fig. 7C). This suggests that although the Golgi localization observed with orthologues of the protein is conserved for MDV pUL51, the determinants for this localization are not exclusively present on the protein itself and that other viral proteins other than pUL7 are probably required.

pUL51 localization to mitochondria was observed in transfected fibroblasts (Fig. 6A and 7A) and the protein was relocalized in the cytoplasm and in the nucleus upon expression of pUL7, a feature that involved the first 159 residues of pUL51 (Fig. 6B). In keratinocytes transfected with pUL51-myc, the protein localized essentially to lipid droplets but could also be occasionally observed in mitochondria whereas pUL51TAP localized mostly in mitochondria and rarely to lipid droplets (Fig. 12B). In keratinocytes, co-expression of pUL51TAP with pUL7 led to relocalization of pUL51 from mitochondria to the cytoplasm whereas it had no effect on pUL51-myc localization to lipid droplets (Fig. 8). Altogether, these observations suggest that MDV pUL51 localization to mitochondria could be artefactual, probably through self-association as suggested by Butt et al. (20), a feature that could be lifted by the interaction with pUL7.

Keratinocytes are the most relevant cells when it comes to MDV natural lytic replication cycle. Although our stem cell-derived keratinocyte cell line does not recapitulate all the features of the keratinocyte from the feather follicle, they contain lipid droplets that are a typical component of chicken keratinocytes (21, 24). The association of pUL51 to lipid droplets is coherent with its known affinity for membranes and our own observations that pUL51 was strongly associated with lipid-rich fractions during attempts of purification of the protein from chicken skin (data not shown). Given the role of pUL51 in secondary envelopment and the features the protein shares with ESCRT-III proteins, the localization of pUL51 on lipid droplets in a cell type that is close to the one that naturally produces high quantities of infectious virus leads to the question of whether lipid droplets could be an assembly site for MDV. Answering this question is tricky because MDV assembly in cell culture is very inefficient, making it particularly burdensome to be reliably monitored by electron microscopy. In addition, the absence of a viable MDV recombinant virus encoding fluorescently tagged capsids makes observation by fluorescence microscopy also challenging, as VP5 epitopes are poorly accessible for antibodies on tegumented particles.

Alternatively, because lipid droplets have been recently described as hubs for innate immunity signaling (25), including for Herpesviruses (26), pUL51 could play a role in altering antiviral mechanisms originating from lipid droplets.

In trying to determine the role of pUL51 in MDV cycle, we failed to obtain recombinant viruses either lacking for pUL51, or with a GFP fusion at the N- or C-terminus of the protein. According to protein folding predictions and secondary structure analysis, the nonconserved C-terminal half of HSV-1 pUL51 seems to be disordered, as opposed to the highly conserved N-terminal half that contains the pUL7-interacting domain and whose structure has been partially solved (20). The fact that a MDV recombinant encoding only the conserved N-terminal half of pUL51 (vUL51ΔCt) is not viable indicates that the C-terminus of the protein is indispensable for its essential function(s). It is therefore possible that the C-terminus of pUL51 is involved in essential protein-protein interactions that could be impaired by the fusion of a rather large tag. Roller at al. have shown that the fusion of GFP to the C-terminus of HSV-1 pUL51 results in a defect in viral CCS without affecting viral replication and that the exogenous expression of pUL51GFP had a dominant negative effect on CCS of WT virus (6). The authors also showed that gE was not localized to cellular junctions in the presence of pUL51GFP, although this property alone could not account for the global role of pUL51 in CCS. A similar scenario could be anticipated for MDV, although the interaction between pUL51 and gE remains to be demonstrated as well as the junctional localization of MDV gE in a cell type where junctions are abundant. It is possible that MDV UL51GFP is as affected in CCS as HSV-1 UL51GFP and, for MDV that cannot produce cell-free particles in cell culture, this would result in no infectious virus recovered from transfected cells.

vUL51TAP is a virus that was initially designed to purify protein complexes associated to pUL51. Purification of pUL51TAP from animal tissues failed during the dedicated experiments essentially because, to our surprise, only very limited amounts of infected material could be recovered from the skin of vUL51TAP-infected animals as opposed to vUL51TAPiSTOP animals. vUL51TAP was therefore a useful surrogate of a functional mutant to study the role of pUL51 during infection of chickens. It is remarkable that although vUL51TAP is not a virus depleted of pUL51, the fusion of the TAP domain at its C-terminus leads to a dramatic defect in pathogenesis that is stronger than the one observed with a MDV mutant depleted of VP16, a major regulator of the viral cycle for alphaherpesviruses, despite the two viruses being similarly impaired in replication (27). This observation alone emphasizes the vital role of pUL51 for MDV and potentially for other Herpesviruses *in vivo* and indicates that the almost complete absence of pathogenesis of vUL51TAP is not only due to its defect in replication.

In comparison, the defect of vUL51TAP in CCS in cell culture is remarkably moderate. Although vUL51TAP is strongly attenuated *in vivo*, pUL51TAP localizes like pUL51-SHA in infected chicken fibroblasts, contrary to HSV-1 pUL51GFP which does not localize to the Golgi, whereas unmodified HSV-1 pUL51 does (6). In addition, pUL51TAP is relocalized away from mitochondria in the presence of pUL7 in fibroblasts and keratinocytes, which indicates that the interaction between pUL51 and pUL7 is unaffected by the TAP fusion. Localization of pUL51TAP to lipid droplets of keratinocytes infected with vUL51TAP could not be observed, which could indicate a lower affinity for this compartment due to the mutation, in line with the observation that pUL51TAP barely localized to droplets in transfected keratinocytes, as opposed to pUL51-myc. This could be significant *in vivo*, although in this case the mutation should affect stages of viral replication or assembly in the skin and not in the PBMC. It is thus unlikely that the phenotype observed with vUL51TAP *in vivo* is linked only to a cellular mislocalization of the mutant protein, although this remains to be tested in relevant PBMCs such as T-lymphocytes.

In conclusion, this study demonstrates the essential role of pUL51 in the biology of MDV and its affinity for lipid droplets in chicken keratinocytes. Importantly, it shows that the protein bears a function that is critical for pathogenesis that is probably localized on its nonconserved C-terminus. This function remains to be determined, but it could be critical for viral transmission from infected circulating lymphocytes to skin keratinocytes through cellular contacts whose nature remains to be identified. Indeed,

these contacts could be distinct from the well-characterized cellular junctions present in established monolayers of fibroblasts. This could explain why the moderate effect of the UL51TAP fusion in CCS in cell culture translates into a dramatic effect on viral spread *in vivo* despite a comparatively moderate effect on replication.

MATERIALS AND METHODS

Plasmids and BACs. All recombinant bacterial artificial chromosomes (BACs) used in this study were derived from the repaired rRB-1B BAC which contains the genome of the very virulent strain RB-1B of MDV as previously described (28, 29). All mutations were introduced into the BAC using the two-step Red recombination technology (30) yielding BACs rUL51M30STOP, rUL51-GFP, rGFP-UL51, rUL51TAP, rUL51TAPiSTOP, rTK_TAP, rUL51SHA, rTK_GFP-SHA, rUL51ΔCt, and rUL51ΔCt-repair.

Plasmids used as templates for the initial PCRs and the sequences of primers used for recombination, cloning PCR, RT-PCR, and quantitative PCR are listed in Table 2. The pEP-GFPin plasmid was a kind gift of Klaus Osterrieder and Benedikt Kaufer (Freie Universität Berlin, Germany). Plasmids pKANinSHA and pKANinTAP were designed by the laboratory and synthetized by GeneArt (Invitrogen). pKANinSHA introduces a linker of five residues (PSRSH) between the target sequence and the SHA sequence and between SHA and the stop codon (LGLMG). Mutations and junctions between viral proteins and tags were verified by sequencing.

The UL51 ORF and its derived fragments 1-159 and 160-end were amplified from rRB-1B using specific primers and cloned into pcDNA3-V5 and pcDNA3-myc using restriction sites HindIII and BamHI. The resulting plasmids were named pUL51-V5, pUL51-myc, pUL51 1–159-V5, and pUL51 160-end-V5 and encoded pUL51 full-length or the designated fragment with a V5 tag or a myc tag at the C-terminus of the protein.

Restriction fragment length polymorphism analysis. A total of 1 μg of BAC DNA was digested with 10 units of NdeI (Promega) for 1 h 30 min at 37°C. DNA was then loaded onto a 0.6% agarose gel in Tris-Borate-EDTA (TBE) buffer preloaded with ethidium bromide and electrophoresis was carried out for 5 h at 50V (35 mA). The profiles obtained were compared to the theoretical profiles generated using pDRAW32 software (v1.1.147 for Windows, Acaclone software) with the following parameters: gel = 0.5%, minimum size cut-off = 500 bp, DNA MW-marker=SmartLadder (Eurogentec).

Cells and viruses. Primary CESCs were obtained from 12-day-old specific pathogen-free (SPF) White Leghorn embryos as described previously (31) and maintained in William's modified E medium containing 1.5% chicken serum and 1% fetal calf serum. These cultures contain mainly dermal fibroblasts and some myoblasts. Chicken keratinocytes derived from chicken embryonic stem cells were used, maintained, and infected as previously described (21, 32). Keratinocytes were transfected by electroporation using the Neon Transfection System (Invitrogen) using 0.5 μg of plasmid and the following parameters: pulse voltage: 1600 V, pulse width: 10 ms, number of pulses: 3. Cells were fixed and processed for antibody labeling no more than 20 h later to limit protein mislocalization due to overexpression.

ESCDL-1 cells are derived from chicken embryonic stem cells and have been characterized and previously validated for MDV replication (33). These cells, which are fully permissive to MDV, can be efficiently transfected by standard methods such as lipofection, as opposed to CESCs. 10^6 cells were transfected using 5 μL of Lipofectamine 2000 (Invitrogen) and 0.5 μg of each plasmid.

Recombinant viruses were all derived from the cloned repaired genome of the very virulent strain RB-1B. They were obtained after transfection of 5.10^6 CESCs with 2 to 4μg of BAC DNA by electroporation using the Amaxa Nucleofector apparatus (program F024) with the Basic Nucleofactor Kit for Primary Mammalian Fibroblasts (Lonza). After 4 days of incubation, viral plaques could be observed. Viruses obtained from the repaired rRB-1B BAC, the rUL51TAP, rUL51TAPiSTOP, rTK_TAP, rUL51SHA, rTK_GFP-SHA, rUL51ΔCt, and rUL51ΔCt-repair BACs were named vRB1B, vUL51TAP, vUL51TAPiSTOP, vTK_TAP, vUL51SHA, vTK_GFP-SHA, vUL51ΔCt, and vUL51ΔCt-repair, respectively.

Viruses used in this study were not passaged more than three times and only on CESCs.

Antibodies. The following primary monoclonal antibodies were used: anti-VP5 MDV (clone F19) (34), anti-gB MDV (clone K11) (28), anti-VP22 MDV (clone B17) (35), anti-ICP4 MDV (clone E21) (28), anti-HA (clone 2-2.2.14, Thermo Fisher Scientific), anti-V5 (#46-0705, Invitrogen), and anti-myc (clone 9E10, Sigma). In addition, a rabbit anti-grasp65 antibody (a gift from V. Malhotra) or a mouse anti-58K (anti-Formimidoyltransferase cyclodeaminase or FTCD) (36) antibody (#58K-9, Novus) were used to label the Golgi apparatus. When specified, a rabbit anti-goat AlexaFluor488 antibody (Sigma) was used to directly label proteins associated with TAP. For UL51TAP-V5 construct, a rabbit anti-V5 antibody (Invitrogen, #PA1993) was used when specified.

Western blots. For Western blot assays, cellular extracts were obtained by dilution of the cell pellet (approximatively 3.10^6 cells) in 90 μL of PBS and addition of 30 μL of 4x Laemmli buffer. In total, 15 μL were loaded on a 10% SDS-PAGE. Proteins were transferred onto Porablot nitrocellulose membranes (Macherey-Nagel) which were probed with a monoclonal antibody against MDV VP5 (clone F19) and a rabbit anti-goat peroxidase-conjugated antibody to detect the TAP tag. Horseradish peroxidase-conjugated goat anti-mouse antibody (Sigma) was used for secondary detection of VP5 in combination with the Immobilon Western HRP substrate (Millipore).

Immunofluorescence. Cells were washed twice with PBS and fixed with 4% paraformaldehyde at room temperature. Fifteen minutes later, cells were washed once with PBS and incubated 15 min at room temperature with 0.1% Triton X-100 diluted in PBS supplemented with 1% goat serum for blocking aspecific antigenic sites, except when labeling of TAP proteins was required (see below). After an additional wash with PBS, cells were incubated with primary antibodies diluted 1:1,000 (1:200 for 58K) in PBS

TABLE 2 List of oligonucleotides used in this study

Primer name	Role	Sequence	Template	BAC	Source template
vUL51_M30STPf	Construction of rUL51M30STOP	ataaacaattgtctgcatcatcttctactgataaagcttaacatcgtct cagggaggcggtaggatgacgacgataagtaggg	pEP-KAN-S	rRB-1B	K. Osterrieder & B. Kaufer
vUL51_M30STPfr	Construction of rUL51M30STOP	AGAATGTTAACGGCATGGACCGCCTCCCTGAGACGATGTTAAG CTTTATCAGTAGAAGATGacaaccaattaaccaattctgattag	pEP-KAN-S	rRB-1B	K. Osterrieder & B. Kaufer
vUL51_GFPCf	Construction of rUL51-GFP	TACAACAATAAACGAAACATACTCGAGAGTATTTGC TTCTTTCTTTATTActtgtacagctcgtccatgccgag	pEP-GFPin	rRB-1B	K. Osterrieder & B. Kaufer
vUL51_GFPCr	Construction of rUL51-GFP	ATTGCCCACCAGTTAAGTTTTCTAGGGAAAATAATC TCATTACCGAATTAgtgagcaagggcgaggagctgttc	pEP-GFPin	rRB-1B	K. Osterrieder & B. Kaufer
vUL51_GFPNf	Construction of rGFP-UL51	TTATATTCTGCTTTGAGTCTTCTGTAGTCGTATGTTC TTGAGCTGGTTTGcttgtacagctcgtccatgccgag	pEP-GFPin	rRB-1B	K. Osterrieder & B. Kaufer
vUL51_GFPNr	Construction of rGFP-UL51	AGTCATCACTTTCGAGCGTATCGGATATAGACGAAAATCTCG CCATAATGgtgagcaagggcgaggagctgttc	pEP-GFPin	rRB-1B	K. Osterrieder & B. Kaufer
vUL51_H161STPf	Construction of rUL51ΔCt	GCGATATAGCACTGGTGGAGAGAGCGTTGGGCTTAACGtaaCCACATA ATGAGAGATCGCCaggatgacgacgataagtaggg	pEP-KAN-S	rRB-1B	K. Osterrieder & B. Kaufer
vUL51_H161STPfr	Construction of rUL51ΔCt	GACTCGTCCATTGATGCGGGCGATCTCTCATTATGTGGTTACGTTAAGCCC AACGCTCTCTacaaccaattaaccaattctgattag	pEP-KAN-S	rRB-1B	K. Osterrieder & B. Kaufer
vUL51_revSTP161Hf	Construction of rUL51ΔCt-repair	GCGATATAGCACTGGTGGAGAGAGCGTTGGGCTTAACGcatCCACATAATGAGA GATCGCCaggatgacgacgataagtaggg	pEP-KAN-S	rUL51ΔCt	K. Osterrieder & B. Kaufer
vUL51_revSTP161Hr	Construction of rUL51ΔCt-repair	GACTCGTCCATTGATGCGGGCGATCTCTCATTATGTGGaTgCGTTAAG CCCAACGCTCTCTacaaccaattaaccaattctgattag	pEP-KAN-S	rUL51ΔCt	K. Osterrieder & B. Kaufer
vUL51_SHACf2	Construction of rUL51SHA	ATTGCCCACCAGTTAAGTTTTCTAGGGAAAATAATCTCATTACCGA ATTACCGTCAAGGCCGCATTAC	pKANinSHA	rRB-1B	This study
vUL51_SHACr2	Construction of rUL51SHA	TACAACAATAAACGAAACATACTCGAGAGTATTTGCTTCTTTCT TTATTAGCCCATGAGGCCCAGTTT	pKANinSHA	rRB-1B	This study
vUL51_TAPCf	Construction of rUL51TAP	ATTGCCCACCAGTTAAGTTTTCTAGGGAAAATAATCTCATTACCGAA TTAGAAAAGAGAAGATGGAAAAAGAATTTC	pKANinTAP	rRB-1B	This study
vUL51_TAPCfr	Construction of rUL51TAP	ATTGCCCACCAGTTAAGTTTTCTAGGGAAAATAATCTCATTACCGAATT AGAAAAGAGAAGATGGAAAAAGAATTTC	pKANinTAP	rRB-1B	This study
vUL51istp_TAPCf	Construction of rUL51TAPiSTOP	GCCCACCAGTTAAGTTTTCTAGGGAAAATAATCTC ATTACCGAATTATAAaggatgacgacgataagtaggg	pEP-KAN-S	rUL51TAP	K. Osterrieder & B. Kaufer
vUL51istp_TAPC2r	Construction of rUL51TAPiSTOP	TTGGCTGCTGAGACGGCTATGAAATTCTTTTTCCATC TTCTCTTTTCCATacaaccaattaaccaattctgattag	pEP-KAN-S	rUL51TAP	K. Osterrieder & B. Kaufer
vTKGFP_SHAf2	Construction of rTK_GFP-SHA	agttcgtgaccgccgccgggatcactctcggcatggacgagctgt acaagCCGTCAAGGCCGCATTAC	pKANinSHA	rTK_GFP	This study
vTKGFP_SHAr2	Construction of rTK_GFP-SHA	ATAAACAAGTTAACGTCGACCCGGGTACCTCTAGA TCCGCTAGCGCTTTAGCCCATGAGGCCCAGTTT	pKANinSHA	rTK_GFP	This study
vTK_TAPf	Construction of rTK_TAP	cacttcgcatattaaggtgacacgcgcggcctcgaacacagctgcaggccatg GAAAAGAGAAGATGGAAAAAGAATTTC	pKANinTAP	rRB-1B	This study
vTK_TAPr	Construction of rTK_TAP	ACAAGTTAACGTCGACCCGGGTACCTCTAGATCCGCTAGCGC TTTACTTGTCAGGTTGACTTCCCCGCGGAATTC	pKANinTAP	rRB-1B	This study
UL51_HindIIIf	Const. with UL51, UL51 1-159, UL51TAP	CTCAAGCTTATGCAAACCAGCTCAAGAACATAC	rRB-1B		
UL51_noSTP_BamHIr	Const. with UL51 and UL51 160-end	TCTGGATCCTAATTCGGTAATGAGATTATTTTCCC	rRB-1B		
UL51L159_BamHIr	Construction of pUL51 1-159-V5	TGGGGATCCTAAGCCCAACGCTCTCTCCACC	rRB-1B		
UL51T160_HindIIIf	Construction of pUL51 160-end-V5	GCGAAGCTTATGACGCATCCACATAATGAGAGATC	rRB-1B		
UL7_EcoRI + 1f	Construction of pmyc-UL7	GGCGAATTCGGAAGAAGAAATGACTTCCATTC	rRB-1B		
UL7_EcoRIf	Construction of pV5-UL7	GGCGAATTCGAAGAAGAAATGACTTCCATTC	rRB-1B		

(Continued on next page)

TABLE 2 (Continued)

Primer name	Role	Sequence	Template	BAC	Source template
UL7_XhoIr	Construction of pmyc-UL7 and pV5-UL7	TTTCTCGAGTCATTTTTGGTATGTGTGAAATAAAC	rRB-1B		
TAPtagCt_BamHIr	Construction of pUL51TAP-V5	TCTGGATCCTCAGGTTGACTTCCCCGCGG	rUL51TAP		
UL50RT_f	RT-PCR on UL50	GATATGTATGTATGGACGACTC			
UL50RT_fr	RT-PCR on UL51	CGCTGCTGTAAGCTTCTGTATC			
UL52RT_f	RT-PCR on UL52	CATACGTATATGAGCATATAC			
UL52RT_fr	RT-PCR on UL52	GACATTTCGAGTCAATATCTAC			
UL18_RTf	RT-PCR on UL18	CAAATGCCCCCTCCTACCAG			
UL18_qPCRr	RT-PCR on UL18	CGCTTTTATATTGGCAGGGC			
iNOSf	qPCR - detection of cellular DNA	GAGTGGTTTAAGGAGTTGGATCTGA			
iNOSr	qPCR - detection of cellular DNA	TTCCAGACCTCCCACCTCAA			
ICP4f	qPCR - detection of viral DNA	TTTCTAGCAAGGAGCGACGC			
ICP4r	qPCR - detection of viral DNA	CGTACTTGCGCTTACGGGAA			
iNos_probe	qPCR - detection of cellular DNA	CTCTGCCTGCTGTTGCCAACATGC			
ICP4_probe	qPCR - detection of viral DNA	CTGCCCAGTCTAGTACCCCTTCTGATATTGGTG			

at room temperature. One hour later, cells were washed three times with PBS and incubated with secondary antibodies diluted in PBS. Secondary antibodies used were Alexa Fluor 488-, 555-, 594-, or 647-conjugated goat anti-mouse and Alexa Fluor 488-, 555-, 594-, or 647-conjugated goat anti-rabbit antibodies (Molecular Probes). The incubation was done as for primary antibodies and cells were then washed three times with PBS. When needed, 4,4-difluoro-1,3,5,7,8-pentamethyl-4-bora-3a,4a-diaza-s-indacene (BODIPY 493/503, Molecular Probes) was added to the cells to a final concentration of 2 μM for 15 min at room temperature to label lipid droplets. MitoTracker Orange (Molecular Probes) was used to label mitochondria according to the manufacturer's instructions.

Cells were washed twice with PBS before being mounted on slides using a mixture of DABCO-Mowiol supplemented with 5 μg/mL Hoechst (Molecular Probes). In the case of TAP-associated proteins, the TAP tag can bind immunoglobulins via its protein A domain. Therefore, when single labeling was required, TAP proteins were directly stained using a rabbit anti-goat Alexa488-conjugated antibody. When double labeling was required, TAP proteins were stained using a V5 rabbit antibody (even though the V5 tag could be absent) and a goat anti-rabbit AlexaFluor488 or 555-conjugated antibody. Only after this labeling would goat serum be applied to the cells (2% in PBS for 15 min) so as to saturate any remaining TAP sites. Then the second protein of interest was labeled using the corresponding antibodies diluted in 2% goat serum. Images were obtained either on an Axiovert 200 M inverted microscope (Zeiss) using a 63x Plan-Apochromat objective (NA = 1.4, Zeiss) and Apotome technology or on a Leica SP8 Scanning Confocal inverted microscope using a 100x PL APO objective (NA = 1.4, Leica). Images were processed using Axiovision LE64 software (release 4.9.1, Zeiss), Leica Application Suite X (LAS X, version 3.7.6.25997, Leica), and ImageJ.

Plaque assays. CESCs seeded in 6-well plates were infected with 100 PFU of vUL51TAP, vUL51TAPiSTOP, vTK_TAP, vUL51SHA, or vTK_GFP-SHA and incubated in medium containing 1% carboxy-methylcellulose to prevent the formation of secondary plaques. Cells were fixed 4 days later with 4% paraformaldehyde and permeabilized with 0.1% Triton X-100. Cells were then blocked using 1% of bovine serum albumin (Fraction V, GE Healthcare) for 20 min at room temperature. Plaques were labeled using a mix of monoclonal antibodies directed against gB, ICP4 and VP22 and Alexa Fluor 488-conjugated (vUL51TAP, vUL51TAPiSTOP, and vTK_TAP) or Alexa Fluor 555-conjugated (vUL51SHA and vTK_GFP-SHA) goat anti-mouse secondary antibodies (Molecular Probes). Images of at least 50 plaques per condition were obtained on an Axiovert 200 M inverted microscope (Zeiss) using a 5x Fluar long-distance objective (NA = 0.25). The size of plaques was determined manually using Axiovision LE64 software (release 4.9.1, Zeiss).

DNA isolation and quantification of viral genomes by TaqMan qPCR. Venous occipital sinus blood samples were collected into tubes containing 3% sodium citrate. PBMC were isolated using density gradient centrifugation on MSL (Eurobio, France). The DNA extractions were performed using the DNA Purification "Blood or Body Fluids Spin" protocol of the QIAamp DNA minikit (Qiagen, Germany). Incubation time with proteinase K at 56°C was extended from 10 min to 2 h to increase DNA yield.

The feather tip from approximatively three to four growing feathers was manually collected and DNA was extracted using the "tissues protocol" of the QIAamp DNA minikit (Qiagen). Samples were incubated overnight at 56°C with proteinase K to ensure efficient lysis. The same protocol was used to extract DNA from dust samples. DNA concentrations were measured with a NanoDrop One spectrophotometer (Thermo Fisher).

Real-time PCR was performed using TaqMan technology, as previously described (37, 38). Both iNos and ICP4 probes were tagged with FAM-BHQ1. All qPCR were performed independently with 250 ng DNA (100 ng for DNA from dust), 10 pmoles of each gene-specific primer, five pmoles of the gene-specific probe in a 20 μL volume on a CFX96 Real Time C1000 Touch Thermal Cycler (Bio-Rad, Marnes-la-Coquette, France). The results were analyzed using CFX Manager software (version 3.1, Bio-Rad). For each sample, viral DNA (based on ICP4 gene) and cellular DNA (based on iNos) were quantified independently in triplicates. For each sample, the number of MDV genome copies was calculated per 10^6 cells.

Sequence alignment. Sequences of pUL51 were collected from the complete genomes from MDV (GenBank # EF523390), MDV-2 (GaHV3 SB1 strain #HQ840738), HVT (#NC_002641), HSV-1 (#X14112), PrV (#NC_006151), VZV (#NC_001348), and BoHV-1 (#NC_001847) and were aligned using ClustalW and Jalview software (build 2.11.1.7) (39).

Animal experiments. Specific pathogen-free (SPF) and MDV maternal antibody-free White Leghorn chicks (B13/B13 haplotype) of 2 weeks of age were obtained from INRAE animal facilities. Animals were separated into two groups of 15 animals housed in two independent isolation units. Ten animals were inoculated with the virus while five other animals were left uninfected ("contacts") to measure viral transmission. Animals were inoculated by intramuscular injection of 2,000 PFU of vUL51TAP or vUL51TAPiSTOP in 200 μL of William's E medium. Animals with apparent symptoms of the disease were euthanized before death occurred to limit suffering.

Statistics. One-way ANOVAs were used to test for significance with Dunnett's test (multiple samples to one control) or Tukey's (Fig. 5C). For multiple comparison of viral loads (Fig. 10B and C), a one-way ANOVA with Sidak's test was used. Results were considered significant for $P < 0.05$. All statistical analyses were performed using Prism6 software (GraphPad).

Ethical statement. *In vivo* experiments were carried out according to the guidance and regulation of the French Ministry of Higher Education and Research (MESR) and the experimental protocol was approved by the regional ethics committee, CREEA VdL ("Comité d'Éthique pour l'Expérimentation Animale Val de Loire") under number #8723-2017013011386459.

ACKNOWLEDGMENTS

All animal experiments were carried out at the Experimental Infectiology Facilities (PFIE) of INRAE (Nouzilly). We are grateful to Sébastien Lavillate, Arnaud Faurie, and

Mylène Girault for their invaluable help with animal care and handling. Many thanks to Klaus Osterrieder and Benedikt Kaufer (Freie Universität Berlin, Germany) for the kind gift of the pEP-GFPin and pEP-Kan-S plasmids. We acknowledge the help of Ines Delhomme for the construction of vUL51TAP and of Mélanie Chollot for the recovery of vUL51ΔCt-repair from transfected cells.

REFERENCES

1. Calnek BW, Adldinger HK, Kahn DE. 1970. Feather follicle epithelium: a source of enveloped and infectious cell-free herpesvirus from Marek's disease. Avian Dis 14:219–233. https://doi.org/10.2307/1588466.
2. Couteaudier M, Denesvre C. 2014. Marek's disease virus and skin interactions. Vet Res 45:36. https://doi.org/10.1186/1297-9716-45-36.
3. Albecka A, Owen DJ, Ivanova L, Brun J, Liman R, Davies L, Ahmed MF, Colaco S, Hollinshead M, Graham SC, Crump CM. 2017. Dual function of the pUL7-pUL51 tegument protein complex in herpes simplex virus 1 infection. J Virol 91. https://doi.org/10.1128/JVI.02196-16.
4. Klupp BG, Granzow H, Klopfleisch R, Fuchs W, Kopp M, Lenk M, Mettenleiter TC. 2005. Functional analysis of the pseudorabies virus UL51 protein. J Virol 79:3831–3840. https://doi.org/10.1128/JVI.79.6.3831-3840.2005.
5. Nozawa N, Kawaguchi Y, Tanaka M, Kato A, Kato A, Kimura H, Nishiyama Y. 2005. Herpes simplex virus type 1 UL51 protein is involved in maturation and egress of virus particles. J Virol 79:6947–6956. https://doi.org/10.1128/JVI.79.11.6947-6956.2005.
6. Roller RJ, Haugo AC, Yang K, Baines JD. 2014. The herpes simplex virus 1 UL51 gene product has cell type-specific functions in cell-to-cell spread. J Virol 88:4058–4068. https://doi.org/10.1128/JVI.03707-13.
7. Dingwell KS, Brunetti CR, Hendricks RL, Tang Q, Tang M, Rainbow AJ, Johnson DC. 1994. Herpes simplex virus glycoproteins E and I facilitate cell-to-cell spread in vivo and across junctions of cultured cells. J Virol 68:834–845. https://doi.org/10.1128/JVI.68.2.834-845.1994.
8. Dingwell KS, Doering LC, Johnson DC. 1995. Glycoproteins E and I facilitate neuron-to-neuron spread of herpes simplex virus. J Virol 69:7087–7098. https://doi.org/10.1128/JVI.69.11.7087-7098.1995.
9. Schumacher D, Tischer BK, Reddy SM, Osterrieder N. 2001. Glycoproteins E and I of Marek's disease virus serotype 1 are essential for virus growth in cultured cells. J Virol 75:11307–11318. https://doi.org/10.1128/JVI.75.23.11307-11318.2001.
10. Roller RJ, Fetters R. 2015. The herpes simplex virus 1 UL51 protein interacts with the UL7 protein and plays a role in its recruitment into the virion. J Virol 89:3112–3122. https://doi.org/10.1128/JVI.02799-14.
11. McGeoch DJ, Rixon FJ, Davison AJ. 2006. Topics in herpesvirus genomics and evolution. Virus Res 117:90–104. https://doi.org/10.1016/j.virusres.2006.01.002.
12. Jiang HF, Wang W, Jiang X, Zeng WB, Shen ZZ, Song YG, Yang H, Liu XJ, Dong X, Zhou J, Sun JY, Yu FL, Guo L, Cheng T, Rayner S, Zhao F, Zhu H, Luo MH. 2017. ORF7 of varicella-zoster virus is required for viral cytoplasmic envelopment in differentiated neuronal cells. J Virol 91. https://doi.org/10.1128/JVI.00127-17.
13. Raza S, Deng M, Shahin F, Yang K, Hu C, Chen Y, Chen H, Guo A. 2016. A bovine herpesvirus 1 pUL51 deletion mutant shows impaired viral growth in vitro and reduced virulence in rabbits. Oncotarget 7:12235–12253. https://doi.org/10.18632/oncotarget.7771.
14. Schauflinger M, Fischer D, Schreiber A, Chevillotte M, Walther P, Mertens T, von Einem J. 2011. The tegument protein UL71 of human cytomegalovirus is involved in late envelopment and affects multivesicular bodies. J Virol 85:3821–3832. https://doi.org/10.1128/JVI.01540-10.
15. Yanagi Y, Masud H, Watanabe T, Sato Y, Goshima F, Kimura H, Murata T. 2019. Initial characterization of the Epstein(-)Barr virus BSRF1 gene product. Viruses 11:285. https://doi.org/10.3390/v11030285.
16. Womack A, Shenk T. 2010. Human cytomegalovirus tegument protein pUL71 is required for efficient virion egress. mBio 1. https://doi.org/10.1128/mBio.00282-10.
17. Feutz E, McLeland-Wieser H, Ma J, Roller RJ. 2019. Functional interactions between herpes simplex virus pUL51, pUL7 and gE reveal cell-specific mechanisms for epithelial cell-to-cell spread. Virology 537:84–96. https://doi.org/10.1016/j.virol.2019.08.014.
18. Selariu A, Cheng T, Tang Q, Silver B, Yang L, Liu C, Ye X, Markus A, Goldstein RS, Cruz-Cosme RS, Lin Y, Wen L, Qian H, Han J, Dulal K, Huang Y, Li Y, Xia N, Zhu H. 2012. ORF7 of varicella-zoster virus is a neurotropic factor. J Virol 86:8614–8624. https://doi.org/10.1128/JVI.00128-12.
19. Wang W, Fu W, Pan D, Cai L, Ye J, Liu J, Liu C, Que Y, Xia N, Zhu H, Cheng T. 2017. Varicella-zoster virus ORF7 interacts with ORF53 and plays a role in its trans-Golgi network localization. Virol Sin 32:387–395. https://doi.org/10.1007/s12250-017-4048-x.
20. Butt BG, Owen DJ, Jeffries CM, Ivanova L, Hill CH, Houghton JW, Ahmed MF, Antrobus R, Svergun DI, Welch JJ, Crump CM, Graham SC. 2020. Insights into herpesvirus assembly from the structure of the pUL7:pUL51 complex. Elife 9. https://doi.org/10.7554/eLife.53789.
21. Couteaudier M, Trapp-Fragnet L, Auger N, Courvoisier K, Pain B, Denesvre C, Vautherot JF. 2015. Derivation of keratinocytes from chicken embryonic stem cells: establishment and characterization of differentiated proliferative cell populations. Stem Cell Res 14:224–237. https://doi.org/10.1016/j.scr.2015.01.002.
22. Nazerian K, Witter RL. 1970. Cell-free transmission and in vivo replication of Marek's disease virus. J Virol 5:388–397. https://doi.org/10.1128/JVI.5.3.388-397.1970.
23. Menon GK, Brown BE, Elias PM. 1986. Avian epidermal differentiation: role of lipids in permeability barrier formation. Tissue Cell 18:71–82. https://doi.org/10.1016/0040-8166(86)90008-x.
24. Vanhoutteghem A, Londero T, Ghinea N, Djian P. 2004. Serial cultivation of chicken keratinocytes, a composite cell type that accumulates lipids and synthesizes a novel beta-keratin. Differentiation 72:123–137. https://doi.org/10.1111/j.1432-0436.2004.07204002.x.
25. Bosch M, Sanchez-Alvarez M, Fajardo A, Kapetanovic R, Steiner B, Dutra F, Moreira L, Lopez JA, Campo R, Mari M, Morales-Paytuvi F, Tort O, Gubern A, Templin RM, Curson JEB, Martel N, Catala C, Lozano F, Tebar F, Enrich C, Vazquez J, Del Pozo MA, Sweet MJ, Bozza PT, Gross SP, Parton RG, Pol A. 2020. Mammalian lipid droplets are innate immune hubs integrating cell metabolism and host defense. Science 370:eaay8085. https://doi.org/10.1126/science.aay8085.
26. Monson EA, Crosse KM, Duan M, Chen W, O'Shea RD, Wakim LM, Carr JM, Whelan DR, Helbig KJ. 2021. Intracellular lipid droplet accumulation occurs early following viral infection and is required for an efficient interferon response. Nat Commun 12:4303. https://doi.org/10.1038/s41467-021-24632-5.
27. Chuard A, Courvoisier-Guyader K, Remy S, Spatz S, Denesvre C, Pasdeloup D. 2020. The tegument protein pUL47 of Marek's disease virus is necessary for horizontal transmission and is important for expression of glycoprotein gC. J Virol 95. https://doi.org/10.1128/JVI.01645-20.
28. Blondeau C, Chbab N, Beaumont C, Courvoisier K, Osterrieder N, Vautherot JF, Denesvre C. 2007. A full UL13 open reading frame in Marek's disease virus (MDV) is dispensable for tumor formation and feather follicle tropism and cannot restore horizontal virus transmission of rRB-1B in vivo. Vet Res 38:419–433. https://doi.org/10.1051/vetres:2007009.
29. Jarosinski KW, Margulis NG, Kamil JP, Spatz SJ, Nair VK, Osterrieder N. 2007. Horizontal transmission of Marek's disease virus requires US2, the UL13 protein kinase, and gC. J Virol 81:10575–10587. https://doi.org/10.1128/JVI.01065-07.
30. Tischer BK, von Einem J, Kaufer B, Osterrieder N. 2006. Two-step red-mediated recombination for versatile high-efficiency markerless DNA manipulation in Escherichia coli. Biotechniques 40:191–197. https://doi.org/10.2144/000112096.
31. Silim A, El Azhary MA, Roy RS. 1982. A simple technique for preparation of chicken-embryo-skin cell cultures. Avian Dis 26:182–185. https://doi.org/10.2307/1590039.
32. Couteaudier M, Courvoisier K, Trapp-Fragnet L, Denesvre C, Vautherot JF. 2016. Keratinocytes derived from chicken embryonic stem cells support Marek's disease virus infection: a highly differentiated cell model to study viral replication and morphogenesis. Virol J 13:7. https://doi.org/10.1186/s12985-015-0458-2.
33. Vautherot JF, Jean C, Fragnet-Trapp L, Remy S, Chabanne-Vautherot D, Montillet G, Fuet A, Denesvre C, Pain B. 2017. ESCDL-1, a new cell line derived from chicken embryonic stem cells, supports efficient replication of Mardiviruses. PLoS One 12:e0175259. https://doi.org/10.1371/journal.pone.0175259.

34. Dorange F, Tischer BK, Vautherot JF, Osterrieder N. 2002. Characterization of Marek's disease virus serotype 1 (MDV-1) deletion mutants that lack UL46 to UL49 genes: MDV-1 UL49, encoding VP22, is indispensable for virus growth. J Virol 76:1959–1970. https://doi.org/10.1128/jvi.76.4.1959-1970.2002.
35. Dorange F, El Mehdaoui S, Pichon C, Coursaget P, Vautherot JF. 2000. Marek's disease virus (MDV) homologues of herpes simplex virus type 1 UL49 (VP22) and UL48 (VP16) genes: high-level expression and characterization of MDV-1 VP22 and VP16. J Gen Virol 81:2219–2230. https://doi.org/10.1099/0022-1317-81-9-2219.
36. Bashour AM, Bloom GS. 1998. 58K, a microtubule-binding Golgi protein, is a formiminotransferase cyclodeaminase. J Biol Chem 273:19612–19617. https://doi.org/10.1074/jbc.273.31.19612.
37. Jarosinski KW, Yunis R, O'Connell PH, Markowski-Grimsrud CJ, Schat KA. 2002. Influence of genetic resistance of the chicken and virulence of Marek's disease virus (MDV) on nitric oxide responses after MDV infection. Avian Dis 46:636–649 .2.0.CO;2] https://doi.org/10.1637/0005-2086(2002)046[0636:IOGROT]2.0.CO;2.
38. Remy S, Blondeau C, Le Vern Y, Lemesle M, Vautherot JF, Denesvre C. 2013. Fluorescent tagging of VP22 in N-terminus reveals that VP22 favors Marek's disease virus (MDV) virulence in chickens and allows morphogenesis study in MD tumor cells. Vet Res 44:125. https://doi.org/10.1186/1297-9716-44-125.
39. Waterhouse AM, Procter JB, Martin DM, Clamp M, Barton GJ. 2009. Jalview Version 2–a multiple sequence alignment editor and analysis workbench. Bioinformatics 25:1189–1191. https://doi.org/10.1093/bioinformatics/btp033.